Mechanical Systems and Signal Processing, Volume 21, Issue 1, January 2007, Pages 208-233.

A comparative experimental study on the diagnostic and prognostic capabilities of Acoustics Emission, Vibration and Spectrometric Oil Analysis for spur gears

Chee Keong Tan[1], Phil Irving[1] and David Mba[2]

[1] School of Industrial and Manufacturing Science, [2] School of Engineering, Cranfield University, Bedfordshire. MK43 0AL, UK

E-mail :- p.e.irving@cranfield.ac.uk, d.mba@cranfield.ac.uk

ABSTRACT

Prognosis of gear life using the Acoustic Emission (AE) technique is relatively new in condition monitoring of rotating machinery. This paper describes an experimental investigation on spur gears in which natural pitting was allowed to occur. Throughout the test period, AE, vibration and spectrometric oil samples were monitored continuously in order to correlate and compare these techniques to natural life degradation of the gears. It was observed that based on the analysis of r.m.s levels only the AE technique was more sensitive in detecting and monitoring pitting than either the vibration or Spectrometric Oil Analysis (SOA) techniques. It is concluded that as AE exhibited a direct relationship with pitting progression, it offers the opportunity for prognosis.

KEYWORDS

Acoustic Emission, condition monitoring, gear pitting, machine diagnosis, prognosis, Spectrometric Oil Analysis, Vibration analysis

1. INTRODUCTION

Acoustic emission (AE) was originally developed for non-destructive testing of static structures [1], however, over recent years its application has been extended to health monitoring of rotating machines and bearings [2-7]. It offers the advantage of earlier defect detection for gearboxes in comparison to vibration analysis [8-10]. However, on seeded faults in gearboxes, this is not without difficulties [11].

The use of vibration analysis for gear fault diagnosis and monitoring has been widely investigated and its application in industry is well established [12-14]. This is particularly reflected in the aviation industry where the helicopter engine, drive trains and rotor systems are fitted with vibration sensors for component health monitoring. Similarly, Spectrometric Oil Analysis (SOA) has been routinely used for elemental analysis of wear particles, contaminants and additives in lubricants for more than 50 years [15]. Analysis of wear particles can assist in determining the source of wear and the condition of the machine. In the aviation industry, this technique has been successfully employed for condition monitoring of rotating components prior the introduction of vibration monitoring technique. Today, it still serves as a complementary diagnostic tool for most aircraft/helicopter platforms. The basic idea of spectrometry is to identify and quantify wear particles from an oil sample. Typical spectrometers are capable of detecting wear particles of between 5 and 10μm.

In this paper, the authors present results from an experimental programme that observed the relationship between AE, vibration and SOA with natural progressive pitting in a pair of spur gears.

2. BACKGROUND

2.1 Acoustics Emission (AE)

AE is defined as transient elastic waves generated due to a rapid release of strain energy caused by structural alteration in/on a solid material under mechanical or thermal stresses. Primary sources of AE are crack initiation, crack propagation, plastic deformation and friction. AE was originally developed as a method of Non-Destructive Testing (NDT) where it was used to monitor crack initiation, propagation and location. Attempts to apply this technique to condition monitoring started in the late 1960's [16]. Some of the principal advantages of AE include:

a) As AE is non-directional, one AE sensor is sufficient to perform the task compared to other techniques such as vibration monitoring which can require information from three axes.
b) Since AE is produced at microscopic level it is highly sensitive and offers opportunities for identifying defects at an earlier stage when compared to other condition monitoring techniques. A typical example is the proven ability [3] to detect the earliest stages of bearing degradation.

c) As AE only detects high frequency elastic waves, it is insensitive to structural resonances and typical mechanical background noise (<20kHz).

However, the main concern on application of the AE technique is the attenuation of the signal during propagation and as such the AE sensor has to be as close to its source as possible. This limitation may pose a practical constraint when applying this technique to certain rotating machinery.

2.2 AE source during gear meshing

Understanding the source of AE activity at the gear mesh is a fundamental pre-requisite if this technique is to be successfully employed for gear diagnostics and prognostics. Toutountzakis [11] highlighted limitations in the current understanding of the source mechanism of AE during gear meshing. Tan et al [17] ascertained the AE source mechanism through a series of experimental programmes. These experimental programmes consisted of isothermal tests on undamaged gears to explore the effects of rotational speed and applied torque on AE levels. From the isothermal test results, it was observed that variation of the applied torque had a negligible effect on the AE r.m.s levels, similar to the negligible effect of load on film thickness under Elastohydrodynamic Lubrication (EHL) of non-conforming mating surfaces. It also noted that the variation in rotation speed had a more pronounced effect on AE r.m.s levels relative to the load. Tan et al [17, 29] concluded that the source of AE during gear mesh was asperity contact under rolling and sliding of the meshing gear teeth surfaces. These

observations detailed by Tan et al [17, 29] were under isothermal conditions. In conditions other than isothermal, an increase in speed and load will result in increased AE levels [26].

2.3 Vibration characteristics and gear damage

Yesilyurt et al [18] utilised the vibration analysis technique for damage detection and assessment, and stated that gear tooth damage would cause a reduction in tooth stiffness and the extent of this damage could be monitored. Yesilyurt concluded that for distributed damage condition the reduction of tooth stiffness and loss of gear tooth involute profile contribute to the increase in vibration. However, in the case of localised defect, tooth stiffness reduction was the sole contributor to the increase in vibration levels. Choy et al [19] came to a similar conclusion. Drosjack et al [20] presented an experimental and theoretical study on the effect of simulated pits located on the pitch-line using vibration technique. Drosjack concluded that pitting on gear teeth surfaces altered the vibration characteristics via the change in stiffness of the gear teeth.

In summary, the presence of damage such as pitting, either localised or distributed, will alter the stiffness of the gear due to modification of the Hertzian contact zone. In addition, an impulsive reaction between gears that have lost the original involute profile will change the vibration levels from the gears.

3. EXPERIMENTAL SET-UP

The test-rig employed for this experimental work consisted of two identical oil-bath lubricated gearboxes, connected in a back-to-back arrangement, see figure 1. The gear set employed was made of 045M15 steel (without any heat treatment) which had a measured hardness of 137 Hv30. The gears (49 and 65 teeth) had a module of 3 mm, a pressure angle of 20°, and a surface roughness (Ra) of between 2-3 μm. A simple mechanism that permitted a pair of coupling flanges to be rotated relative to each other, and locked in position, was employed to apply torque to the gears.

The AE sensors used for this experiment were broadband type with relatively flat response in the region between 100 KHz to 1MHz. One sensor was placed on the pinion with 49 teeth. And the second AE sensor was located on the bearing casing. The cable connecting the sensor placed on the pinion with the pre-amplifier was fed into the shaft and connected to a slip ring ('IDM' PH-12). This arrangement allowed the AE sensor to be placed as close as possible to the gear teeth. The sensor was held in place with strong adhesive superglue. The output signal from the AE sensors was pre-amplified at 20dB. The signal output from the pre-amplifier was connected (i.e. via BNC/coaxial cable) directly to a commercial data acquisition card.

An accelerometer was fitted onto the bearing casing to record vibration data, see figure 1. The accelerometer used for vibration measurement in this experiment was a resonant type

sensor with a frequency response between 10 Hz and 8000 Hz. The accelerometer was mounted on the base of the bearing casing connecting to the pinion shaft. The accelerometer was connected to a charge amplifier, and the signal output from the pre-amplifier was fed to a commercial data acquisition card.

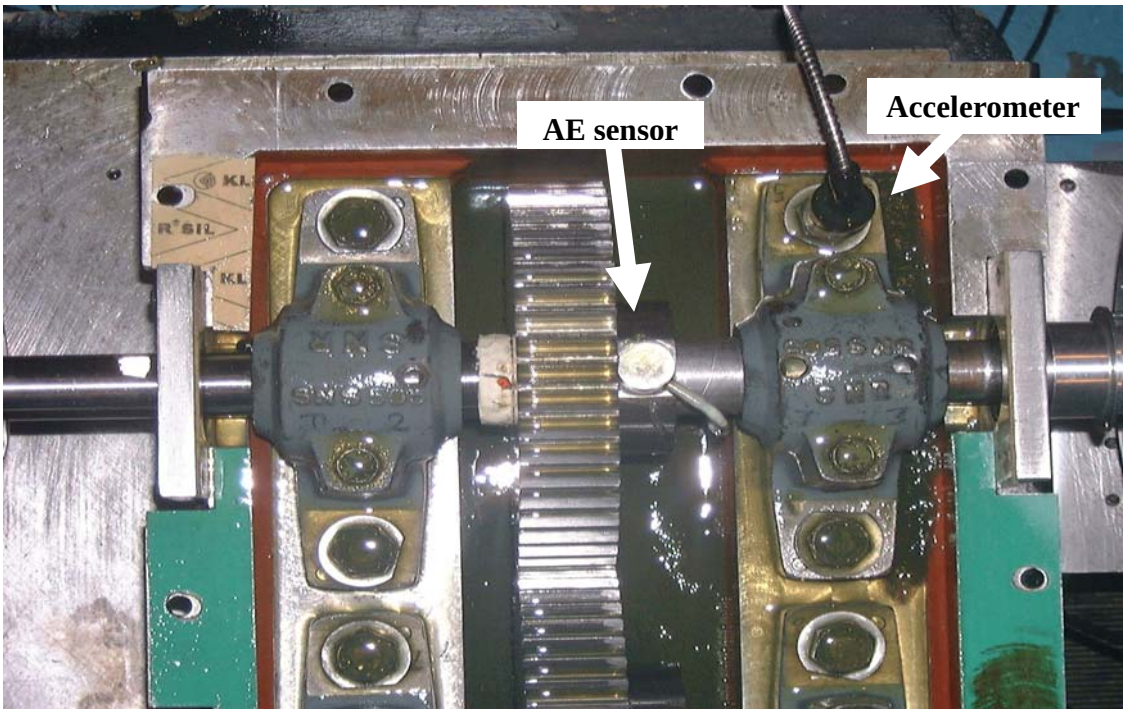

Figure 1 Back-to-back gearbox arrangement with AE sensors and accelerometer

In normal gearbox operation, an anti-wear lubricant is usually employed to prevent or slow down wear on the gear teeth. In order to initiate surface pitting in a relatively short time frame, lubricant oil without anti-wear properties was employed for the accelerated gear fatigue tests; SAE 20W-50. Also, to accelerate the pitting process the face width of the pinion employed was half that of the wheel.

4. EXPERIMENTAL PROCEDURES

The fatigue gear tests were performed at a rotational speed of 745 rpm and applied torques of 220, 147 and 73 Nm. Two tests were undertaken at each torque to ensure repeatability. At regular intervals (ranging from 15 to 55 hours depending on the applied torque levels), visual inspection of gear surface damage was undertaken, oil sump temperatures were measured and oil samples were drawn for SOA (see table 1 and 2).

Table 1 Inspection and SOA collection intervals for all the test conditions

Interval No.	Applied Torque					
	73 Nm		147 Nm		220 Nm	
	Test 1	Test 2	Test 1	Test 2	Test 1	Test 2
	Cumulative inspection time (hours)					
1	0	0	0	0	0	0
2	45	49	24	24	9	17
3	95	96	46	48	20	28
4	145	144	70	72	31	40
5	196	193	94	96	41	52
6	268	241	118	121	54	70
7	353	290	143	145	70	86
8	425	341			91	
9	485	403			116	
10		472				

Table 2 Oil temperatures at respective inspection intervals for all the test conditions

Interval No.	Applied Torque					
	73 Nm		147 Nm		220 Nm	
	Test 1	Test 2	Test 1	Test 2	Test 1	Test 2
	Oil temperatures at respective cumulative inspection times (^{0}C)					
1	19.7	21.7	24.1	22.1	23.1	23.8
2	36.5	37.4	48.0	44.5	60.9	60.5
3	36.3	37.0	50.2	46.7	64.1	61.9
4	38.2	37.6	51.7	48.3	63.8	62.9
5	37.8	39.4	52.8	50.3	65.3	63.8
6	36.2	37.9	54.3	51.3	65.2	63.1
7	36.4	40.2	49.9	51.0	66.0	63.9
8	35.7	41.9			63.0	
9	35.9	40.5			64.0	
10		48.0				

Continuous AE r.m.s values from the bearing casing and pinion gear were calculated in real time by the analogue-to-digital converter (ADC) controlling software. This software employed a hardware accelerator to perform calculations in real time for a programmable time interval set by the user, 10ms in this instance and a sampling interval of 90ms was employed. Anti-aliasing filters were also employed prior to the ADC. Raw vibration

waveforms, sampled at 8192 Hz, were recorded for a period of 1 second at intervals of 30 minutes. Vibration r.m.s values were calculated over the recorded duration (1-second).

During the inspection interval, gear teeth surfaces on both the pinion and gear were visually inspected for pitting or other abnormalities such as scoring and scuffing. The largest pitted area on any single tooth was recorded. The authors set the failure, or test termination, criterion at 50% pitted area of the gear tooth surface area. The visual inspections were performed by two separate inspectors independently and repeated for consistency. This inspection error was determined to be ± 5% of pitted area.

The spectrometer used for SOA is an Atomic Emission type, namely Inductively Coupled plasma (ICP). The analysis was performed by subjecting the oil sample to high voltage plasma which energises the atomic structure of the metallic elements, causing emission of light. The emitted light is subsequently focused into the optical path of the spectrometer and separated by wavelength, converted to electrical energy and measured. The intensity of the emitted light for any element is proportional to the concentration of wear metal suspended in the lubricating fluid. The ICP used for determining levels of Fe elements in the lubricating fluid had an accuracy of ± 3% at an average precision of 95% confidence level.

5. RESULTS

5.1 Pitting Rates

Figure 2 shows percentage of the gear surface pitted area plotted against the test operating time. For each torque condition a linear equation was fitted to both sets of data. The worst fit was at 73 Nm with a correlation coefficient value (R^2) of 0.8696. The gradient values of the equations fitted to each data set represent the pitting rates at each applied torque. These values were 0.45, 0.35 and 0.10 (%/hr) for 220, 147 and 73 Nm respectively. The highest gear teeth pitting rate was observed at 220 Nm (figure 2). With decreasing torque levels the rate of pitting decreased.

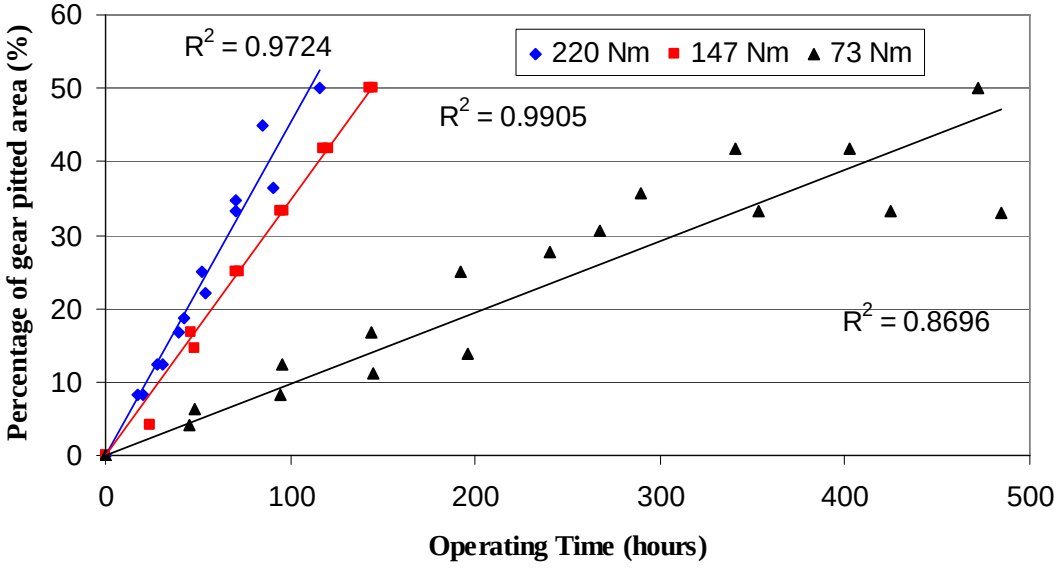

Figure 2 Pitting rates of the test gear under 220, 147 and 73 Nm; 745 rpm

5.2 Data Analysis

All original data from AE, SOA and vibration are presented in figures 3 to 10 (220Nm) and figures 18 to 33 (147 and 73Nm) in appendix B. A few general observations on all torque levels were noted. From figure 3, it can be seen that in one of the tests the AE r.m.s initially decreased, whereas in the other it increased from the start. After approximately 15 hours the AE levels in both tests increased at very similar rates (gradients) but different absolute AE r.m.s values. Figure 4 shows a plot of AE r.m.s versus the percent gear pitted area illustrating a linear relationship between the two for both tests. A totally linear relationship was not mirrored from the AE measurements taken from the bearing casing, see figures 5 and 6. In the latter instance a linear relationship was noted from approximately 15 hours until about 70 hours after which a relatively rapid rise in r.m.s values was noted. The reason AE measurements from the bearing casing were not completely linear, as observed from AE measurements taken from the gear pinion, was attributed to attenuation, increased vibration levels after 70 operational hours (see figure 7) and varying transmission paths through the bearing as a function of roller position. The influence of roller position within the bearing on AE transmission was recently noted by Tan et al [28].

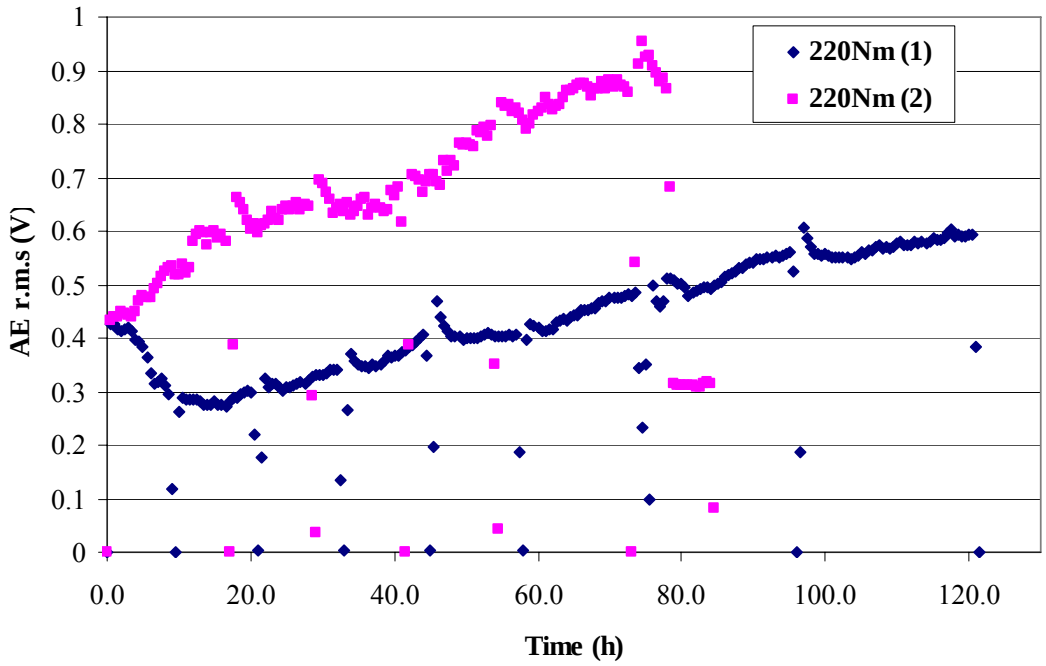

Figure 3 **AE r.m.s against operating time at 220 Nm; 745 rpm**

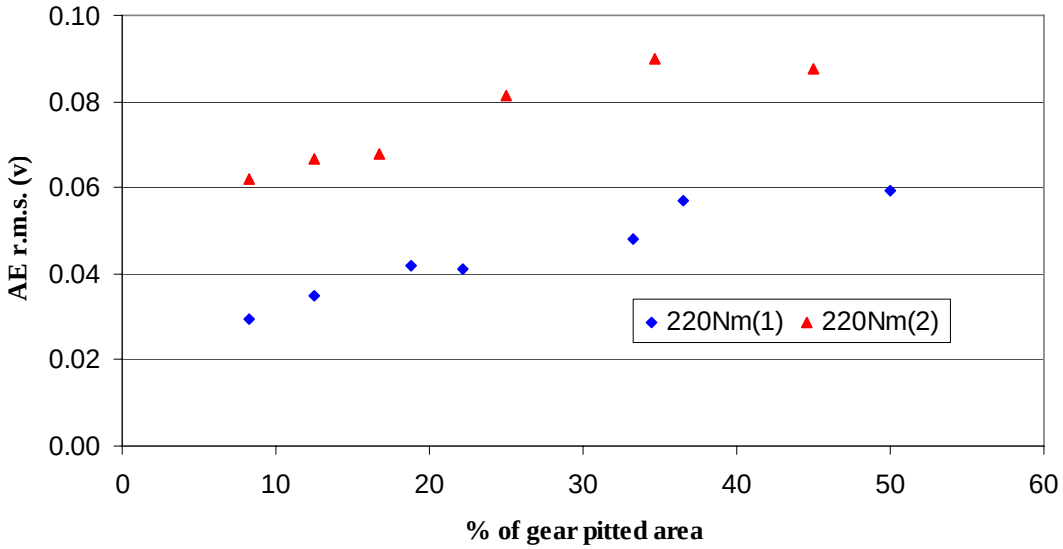

Figure 4 **AE r.m.s against % pitted area; 220 Nm, 745 rpm**

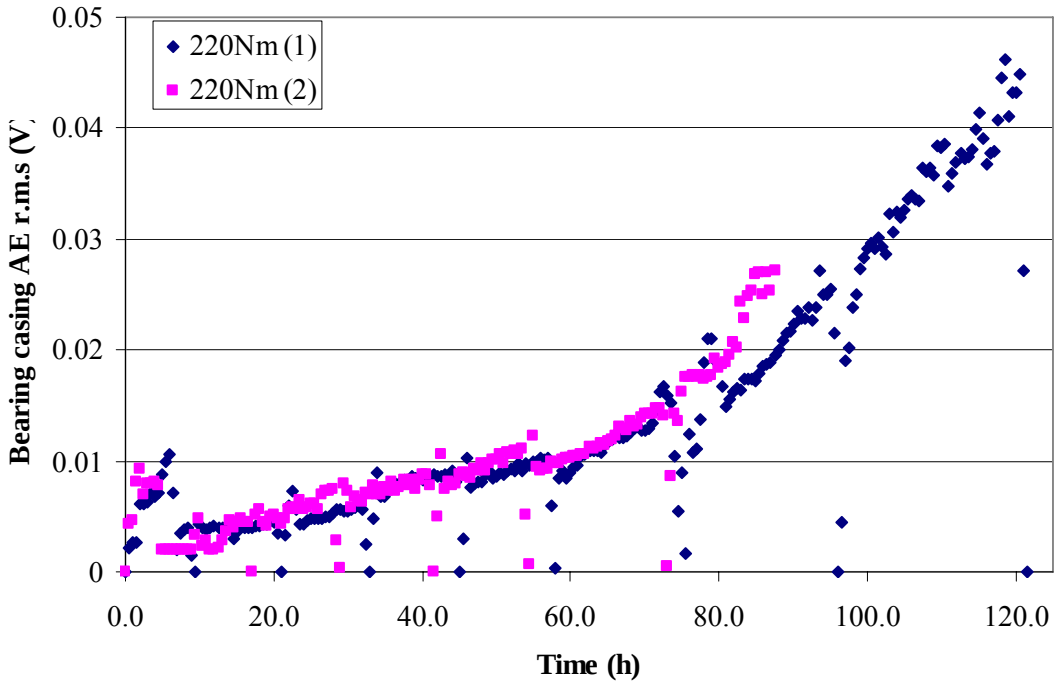

Figure 5 **Bearing casing AE r.m.s against operating time at 220 Nm; 745 rpm**

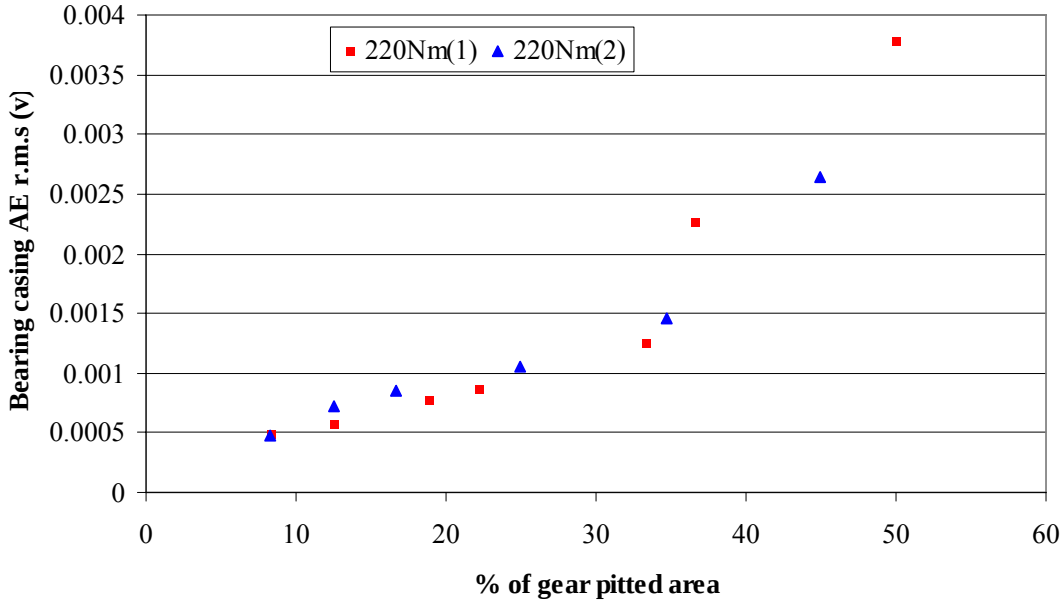

Figure 6 **Bearing casing AE r.m.s against % pitted area; 220 Nm, 745 rpm**

Figure 7 shows vibration r.m.s values against time for the 220Nm test. It demonstrates that the application of the same torque produced similar vibration r.m.s values until 60 hours when the tests departed from each other. Also it was observed that there was an initial increase of vibration level from 0 to between 10 and 15 hours, thereafter the vibration level remained relatively constant until 60 hours. Figure 8 shows the original vibration r.m.s values plotted against percentage of pitted area. Following the run-in period vibration levels remained constant until 25% pitted area, after which levels rose steadily.

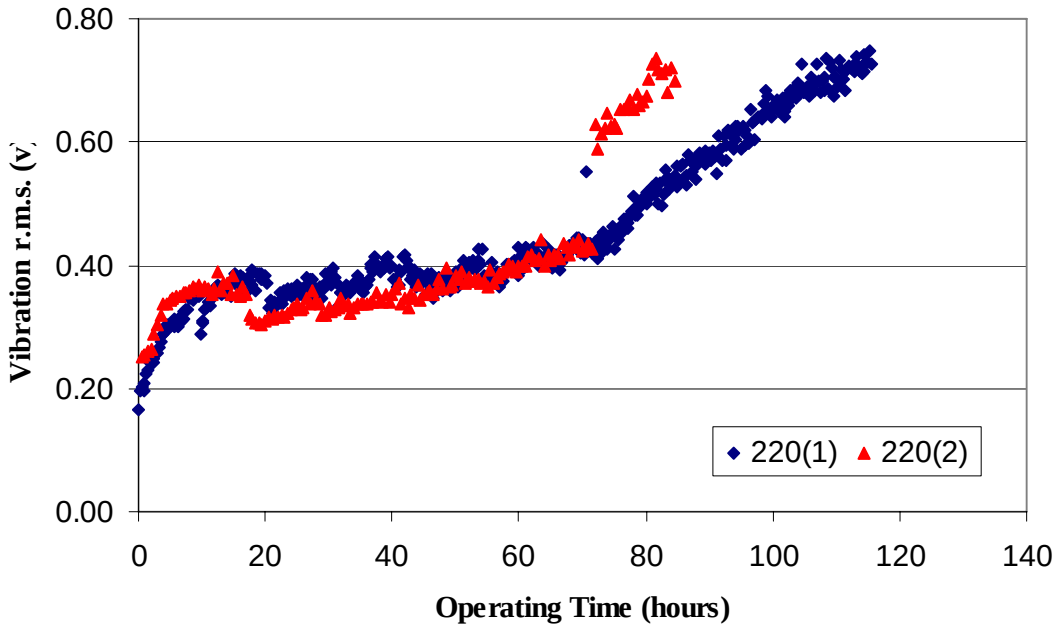

Figure 7 Vibration r.m.s against operating time at 220 Nm; 745 rpm

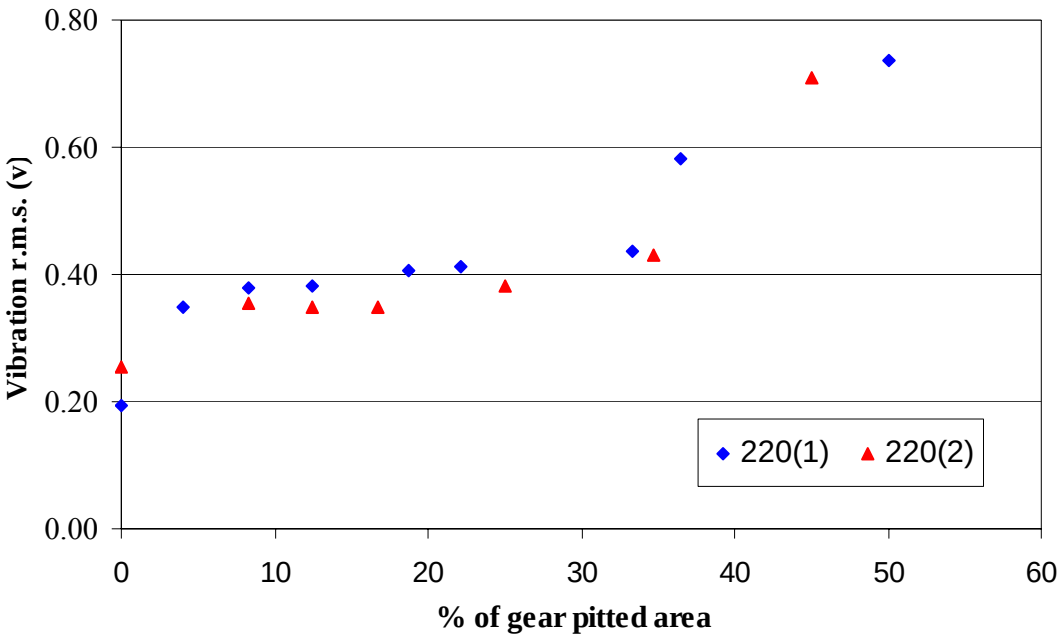

Figure 8 Vibration r.m.s against % pitted area; 220 Nm, 745 rpm

From figure 9 levels of SOA with operating time are presented which show diverging levels after approximately 17 hours of operation. It is interesting to note that though SOA levels for both tests diverged, they maintained an approximately similar overall gradient. Figure 10 shows absolute Fe concentration levels at different percentage pitted areas; the differences between both tests under the same torque can be noted.

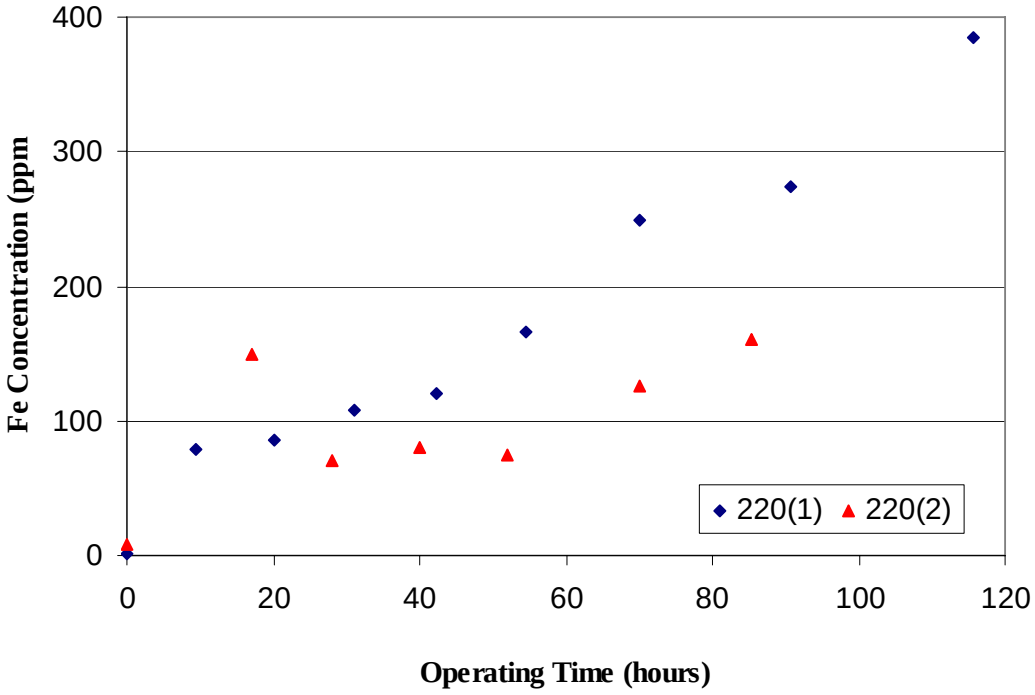

Figure 9 **Fe concentration with correction against operating time at 220 Nm; 745 rpm**

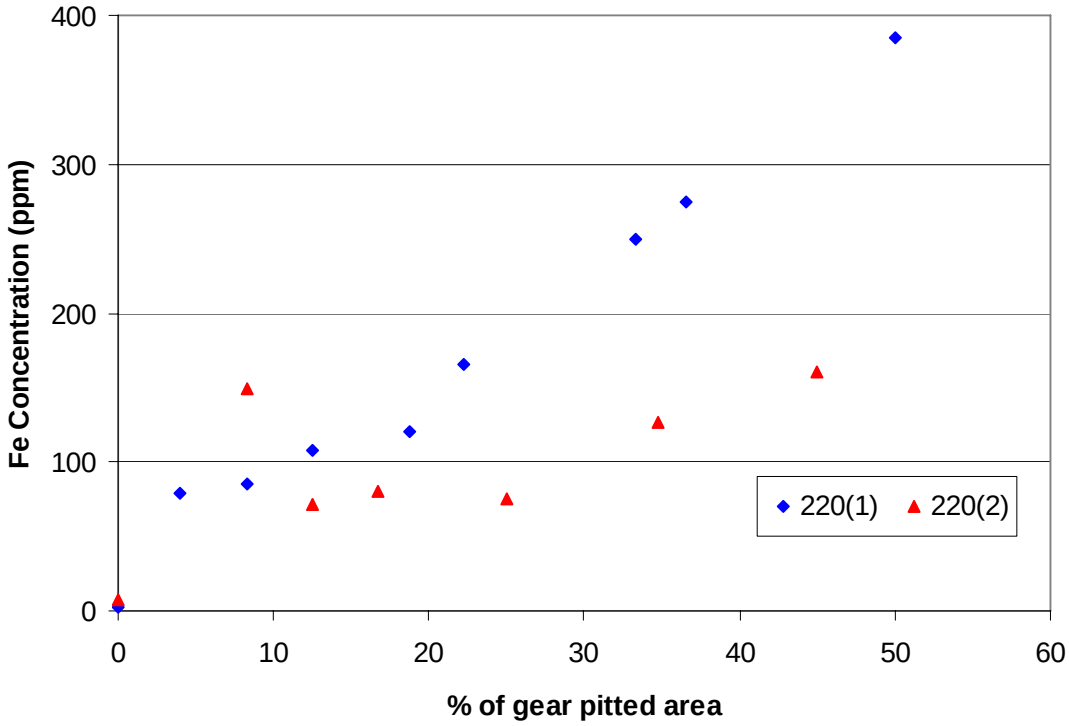

Figure 10 **Fe concentration with correction against % pitted area; 220 Nm, 745 rpm**

The observed pitting progression for all test conditions are summarised in Appendix A which lists all detailed observations of scoring, pitting rates and location of pitting in relation to the gear face area (dedendum, pitch and addendum) as a function of operating time. The experiments revealed that pitting occurred from the dedendum and moved towards the pitch-line. For the higher applied torque conditions (220 and 147 Nm), the pitting always occurred across the face width and was evident on most of the gear teeth. For the light torque condition (73 Nm), pits spread across the face width of the gear teeth at a much slower rate and was localised to only a few teeth. With prolonged operation time, the pitting spread across to other gear teeth. Figures 11 to 13 show the progression

of gear tooth pitting from 6.3% to 41.7% of gear pitted area, under the test condition of 73 Nm and 745 rpm.

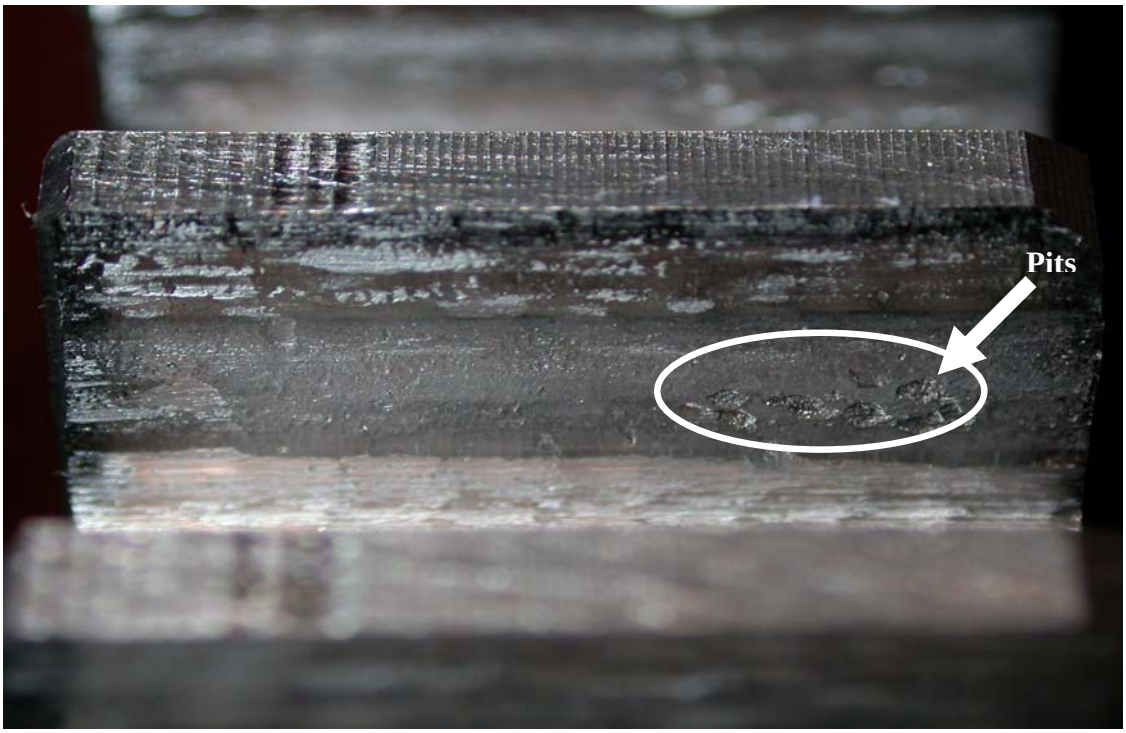

Figure 11 6.3% of gear pitted area at 48.5 hours of operating time; 73 Nm and 745 rpm

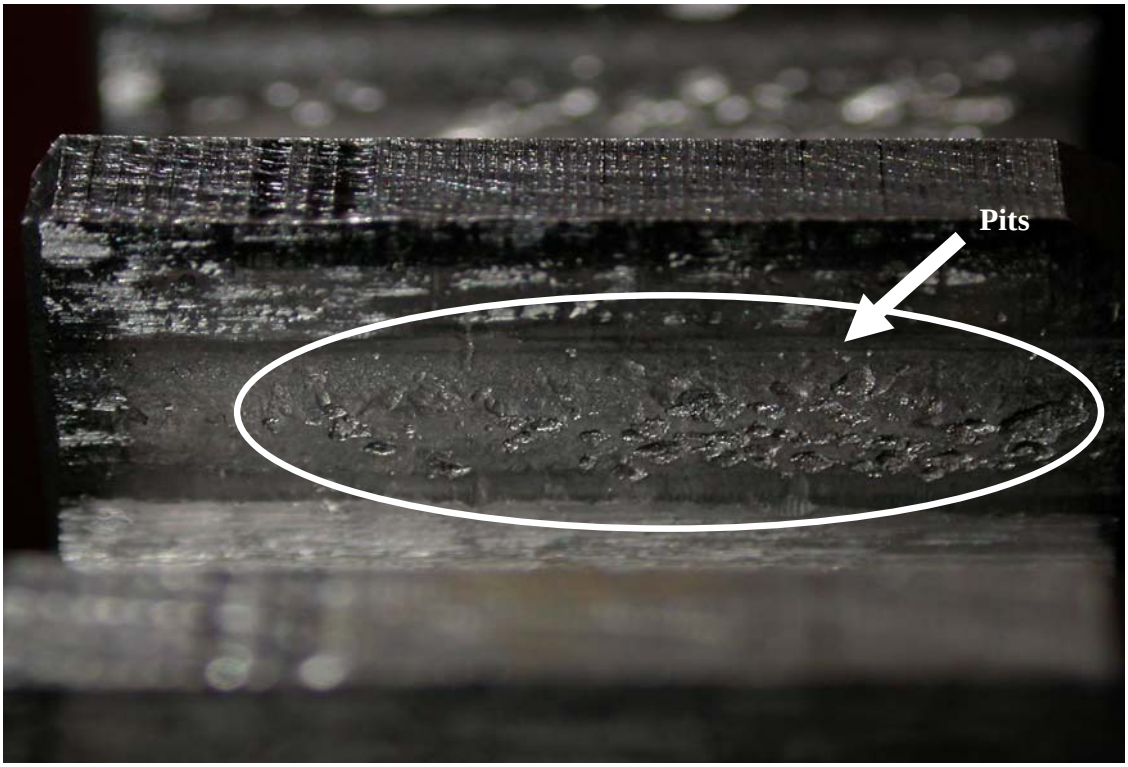

Figure 12 **27.8% of gear pitted area at 240.5 hours of operating time; 73 Nm and 745 rpm**

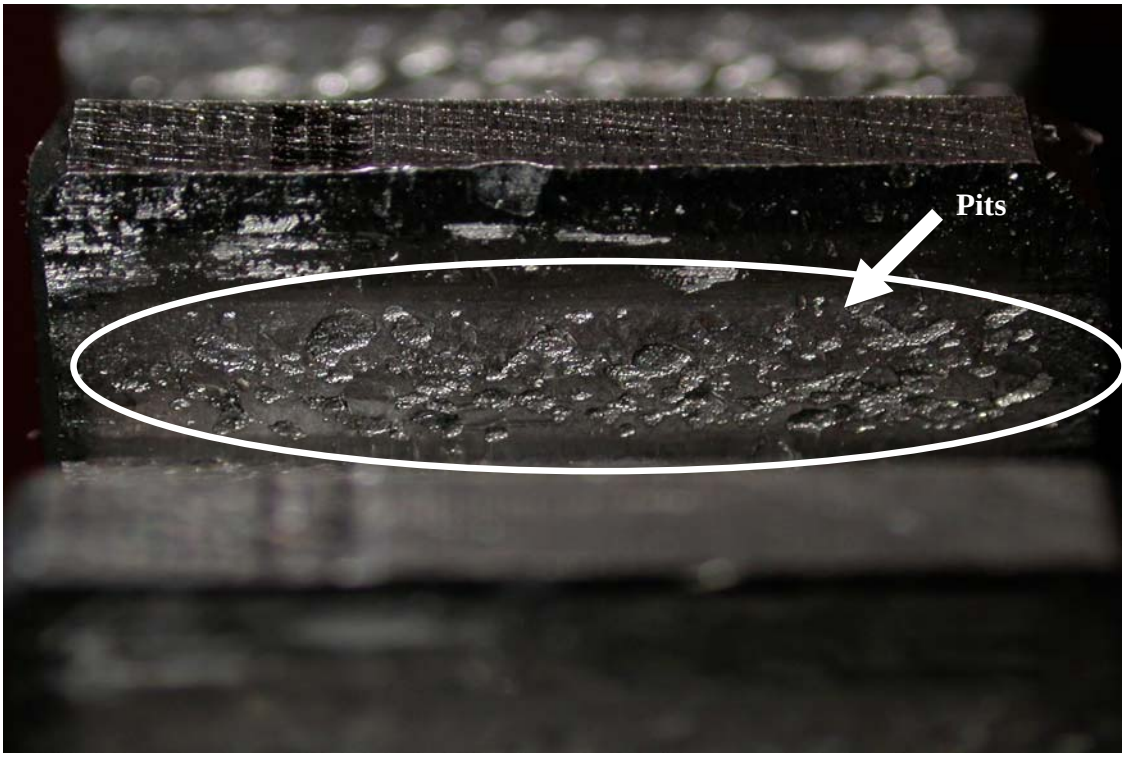

Figure 13 **41.7% of gear pitted area at 402.5 hours of operating time; 73 Nm and 745 rpm**

6. DISCUSSION

6.1 AE and pitting

In relating AE activity to pitting rates cognisance of the effects of surface roughness, lubrication regime, friction and the slide-to-rolling ratio of the meshing gears must be considered. Xiao et al [23] investigated the effect of surface topography on lubricated sliding gear surfaces and noted that friction coefficient of mating surfaces increased with increasing average surface roughness. Diei [24] proposed a relationship between AE

r.m.s and the rate of frictional energy dissipation from sliding contact. In relating AE to sliding friction Dornfeld [26] et al have shown the high sensitivity of AE to sliding speed and applied load. It was noted that the basic mechanism for AE generation during sliding was the elastic deformation of the material at asperity contacts. This deformation was augmented by increased rates (sliding speed), contact forces and lubrication. Furthermore, the relationship between AE and wear of mating surfaces was presented by McBride et al [27] where it was stated that '*This paper shows that asperity contact can be detected by acoustic emission measurements, and that such measurements can provide a vital understanding of the complex wear processes in both dry and lubricated situations'.* Suh [25] defined asperity deformation as the main determinant of friction in metal to metal contact whilst Tan et al [17] concluded that the source of AE during the gear mesh was attributed to asperity contact. Based on the observations of AE activity and pitting progression during this investigation, and conclusions of the various researchers detailed above, the authors postulate that AE levels will increase with increasing gear pitted area. A consequence of the increase in pitted area is an increase of surface roughness and friction, leading to an increase in AE levels. This deduction was confirmed by the observations of AE r.m.s levels from the pinion gear (figures 3, 4 and 18 to 21) which show AE levels increasing with operating time / gear pitted area. However, observations of AE levels from the bearing casing were inconsistent. Whilst at the higher torque value of 220Nm a direct relationship between AE levels and pitting was observed, the AE response at the lower torque values of 147Nm and 73Nm were not sensitive to monitoring the rate of surface degradation.

6.3 Diagnostics and prognostics capabilities

In assessing the diagnostics and prognostics capabilities of the AE, SOA and vibration monitoring techniques for gear teeth surface pitting wear, the following questions arise:

1) Which is the best indicator for monitoring pit growth?
2) How does load affect the various indicators?
3) What is the prognostic potential of these technique?

6.3.1 Which is the best indicator for monitoring pit growth?

Clearly, there existed an initial period during which the gear teeth surface smoothened out, oil sump temperatures increased and dynamic stabilisation of the rotating systems (such as bearing, alignments etc) took place. Because of the complexity involved during this process, it was deemed inappropriate to relate any of the monitoring indicators to this period; 0 to 15hrs. However, after this initial period defined as wear-in, the monitoring indicators behaved differently with pit progressions. As discussed earlier, AE r.m.s levels exhibited a linear relationship with running time (as observed from AE measurements taken from the gear after the run-in period), which was not necessarily the case for vibration, SOA and AE (bearing casing) observations.

6.3.1.1 The AE technique

Throughout the duration of the tests it is believed that there are two processes affecting the generation of AE. Firstly, the wear-in process which causes a smoothing of surface roughness with a consequent decrease in AE levels. The second involves the increased surface roughness due to pitting progression/development which will increase surface roughness and AE levels. At the beginning of the tests AE levels will also be influenced by the oil film temperature and dynamic characteristics of the test-rig arrangement. Increasing oil temperature will lead to a reduction of oil film thickness; this encourages more asperity contacts resulting in increased AE levels. On the other hand, the smoothing of the gear teeth surfaces due to the wear-in process will reduce surface roughness which will result in lower AE levels. Furthermore, the authors postulate that the factors that determine the onset value of the AE level are the initial surface roughness of the gear teeth surfaces, assembly of the gear components and bearings, and, the initial oil temperature.

The two test results at 220Nm, see figure 3, exhibited different trends at the start of the tests; '220(1)' showed decreasing AE levels up to 15 hours operational time, whereas AE level for '220(2)' increased from the start of the test. It is postulated that the difference is due to the balancing process between increasing oil temperature and reducing surface roughness of the gear teeth, which have opposing effects on AE levels. In addition, the authors cannot guarantee that the exact positioning of the gear wheels and clearances

within the gearbox were identical for each test condition; best practice was followed. For this particular test, from about 15 hours, 8% of gear pitted area; the AE r.m.s values increased linearly with increasing running time and pitted area. An important point to note; both test cases exhibit similar gradient from 8% pitted area or 15 hours running time onward. Similar observations were noted for 147 and 73 Nm tests (see figures 18 to 21 of appendix B). The linear relationship between AE levels measured from the sensor placed on the pinion and pit growth rate at all torque conditions was encouraging and emphasised the sensitivity of the AE technique.

Observations of AE activity measured from the bearing casing showed differing correlations between torque levels and pitting wear. At 220Nm, and after 15hours run-in, a linear relationship between AE levels and pit growth was noted until about 70 hours of operation. At this instance the rate of increase in AE r.m.s levels with operating time/wear increased further; deviating from the linear relationship, see figure 5. It is interesting to note that at 70 hours of operation the vibration levels of the bearing casing increased; see section 6.3.1.2 and figure 7. The increase in the rate of increasing AE levels at this instance (70hrs) is attributed to the additional generation of AE from within the bearing as a direct result of increased vibration. This is in addition to the AE generated from the wearing of the gears. At the lower torque levels the observations of AE activity were different to that observed at 220Nm. At the lower torque loads the AE levels remained at electronic noise levels until about 50, 80 and 130 hours, depending on the load and test, after which a sudden increase in AE levels were noted, see figures 22 to 25 of appendix B.

6.3.1.2 The Vibration technique

Figure 9 shows the plot for vibration r.m.s against gearbox operating time under an applied torque of 220Nm. Vibration r.m.s increased from 0 to between 10 to 15 hours, which was indicative of increasing oil temperature (see table 2) and decreasing oil film thickness. As oil film thickness reduced, the damping effect of the oil film between the meshing gear teeth surfaces will reduce resulting in increasing vibration levels. A plateau was observed for the vibration r.m.s between 15 to 55 hours of the running time, even though gear surface pitted area increased to 25%, see figure 10. This showed that vibration technique was unable to monitor the pit grow process until the pit development was advanced. Hence at this point, it can be concluded that AE technique has an advantage over vibration technique in terms of pit growth monitoring. Observations of vibration response at 147Nm and 73Nm, figures 26 to 29 of appendix B, reiterated the observations detailed above. Unfortunately during the second test condition under 147Nm the vibration acquisition system failed, thus only one test result for vibration is available at this condition. In summary, the vibration response increased when minimum criteria of 25% pitted area was reached which is attributed to alterations in the stiffness of the gear due to modification of the Hertzian contact zone. It must be noted that for this particular investigation the gearbox configuration is very simple, on real operational gearboxes as used on helicopters, the detection of pitting would occur later in operational life. This conclusion is attributed to the increased background noise levels and highly complex transmission path from the gears to the sensor.

6.3.1.3 Fe Concentration

As mentioned earlier it is believed that there are two processes operating during the tests. Firstly, the wear-in progress which causes a smoothening of surface roughness, and secondly the increased surface roughness due to pitting progression/development. At the beginning of the tests SOA levels will also be influenced by oil film temperature. An increase in oil temperature will led to a reduction of oil film thickness which will result in increased asperity contact hence increased Fe concentration levels. On the other hand, the smoothening of the gear teeth surface due to the wear-in progress will also result in Fe particle production. Typically the concentration levels increased with operational time and level of applied torque. However, this was not exactly true for the test condition of 73Nm, see figures 9, 10, and 30 to 33 of appendix B. The authors postulate that as the pit rate at 73 Nm test condition is significantly lower than the other tests, the concentration of pit particles within the SOA detectable range may not increase consistently with the operating time. However, when all Fe data are plotted against percentage pitting, see figure 17, more consistent behaviour is obtained after 20% gear pitted area. The unique observation of Fe concentration levels for the first 15 hrs at 73Nm is attributed to the particle generation during wear-in. From this observation it is envisage that for the torque conditions where pit development is slow, wear-in will dominate over particles generated from pits until such a time that pit progress begins.

At the higher applied torque (220 Nm) the averaged absolute value of the Fe concentration was significantly higher than at 147 and 74 Nm; 146.5ppm compared to 43.5 and 24.5ppm respectively.

6.3.1 How does load affect the various indicators?

The influence of torque on these monitoring indicators could provide valuable information on the potential, or limitation, in applying these techniques in practical situations where environmental and operational factors come into play. The load dependency of each indicator was investigated in terms of gearbox operating/running time and percentage of gear pitted area.

6.3.2.1 Gear AE r.m.s

From figure 14 at any particular given operating time, the greater the applied torque the greater the AE r.m.s value. This is due to the fact that the lubricant oil temperature is relatively higher at higher applied torques, which in turn produced a smaller oil film thickness. The average oil temperatures for 220, 147 and 73 Nm were 63.2, 50.0 and 38.3^0C respectively (see table 2). The thinner oil film will result in more asperity contact at the meshing gear teeth surfaces, thus higher AE activity. This will only hold true when the lubricating regime is under partial EHL. It was also observed that the rate of pitting increased at higher torques. In addition, this showed that the AE technique had a good sensitivity to percentage pitted gear area at all torque levels following the wear-in period.

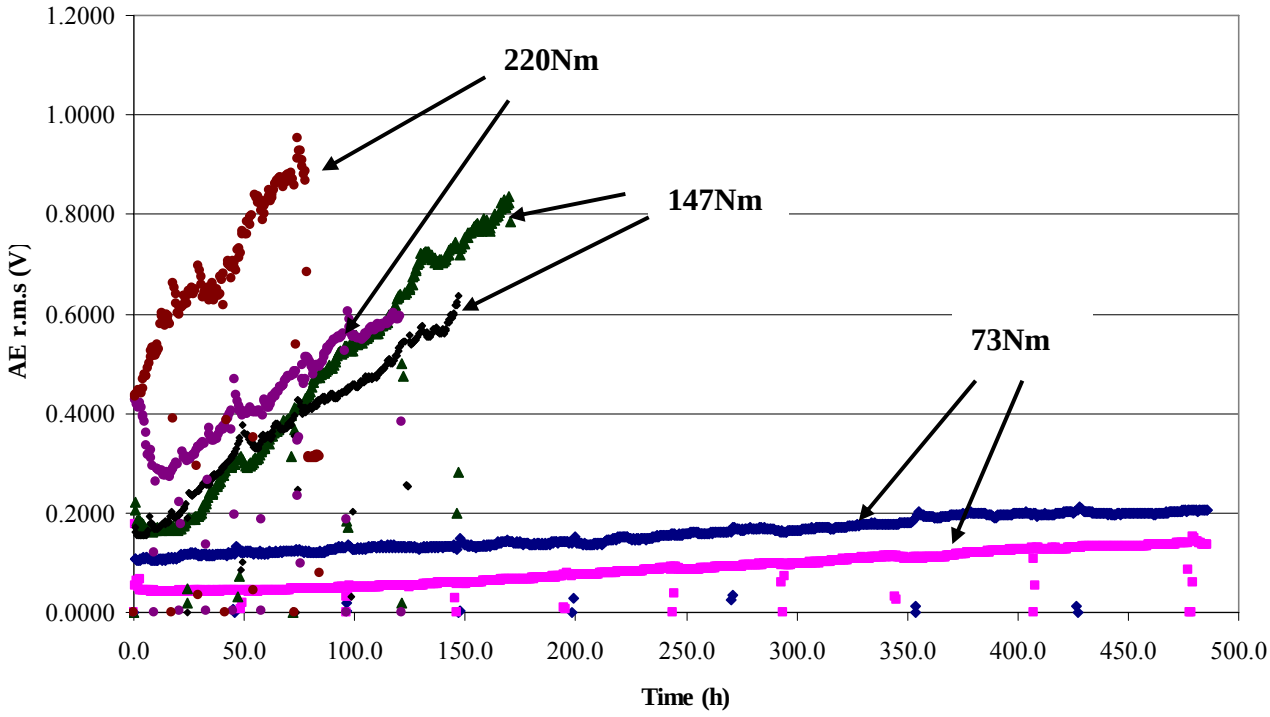

Figure 14 **AE r.m.s against gearbox operating time for various torque conditions at 745rpm**

6.3.2.2 Bearing casing AE r.m.s

From figure 15 at any particular given operating time, the greater the applied torque the greater the AE r.m.s value though this was dependent on the operational time. At 220Nm the rate of increase in levels of AE showed good sensitivity to pitting but this was not the case at the lower torque loads (147 and 73Nm). At 147Nm AE levels remained at electronic noise levels until 50 and 80 hours of operation. At these times AE activity increased as a result of the wear on the gear faces, see figures 22 to 25 of Appendix B. It

is worth stating that the reason for this reduced sensitivity of AE measurements from the bearing casing is attributed to attenuation of the high frequency AE waves. The influence of transmission path (i.e., the location of the roller in the bearing) will also contribute to the reduced sensitivity [28].

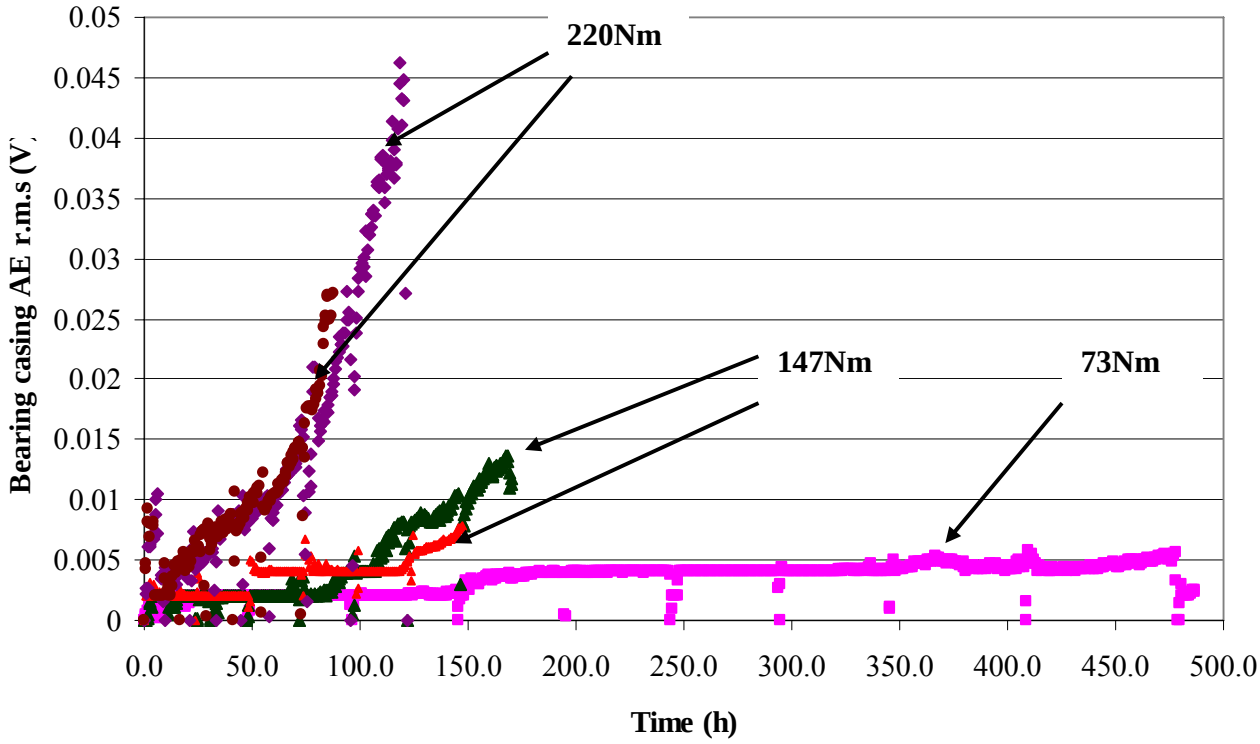

Figure 15 **Bearing casing AE r.m.s against gearbox operating time for various torque conditions at 745rpm**

6.3.2.3 Vibration r.m.s

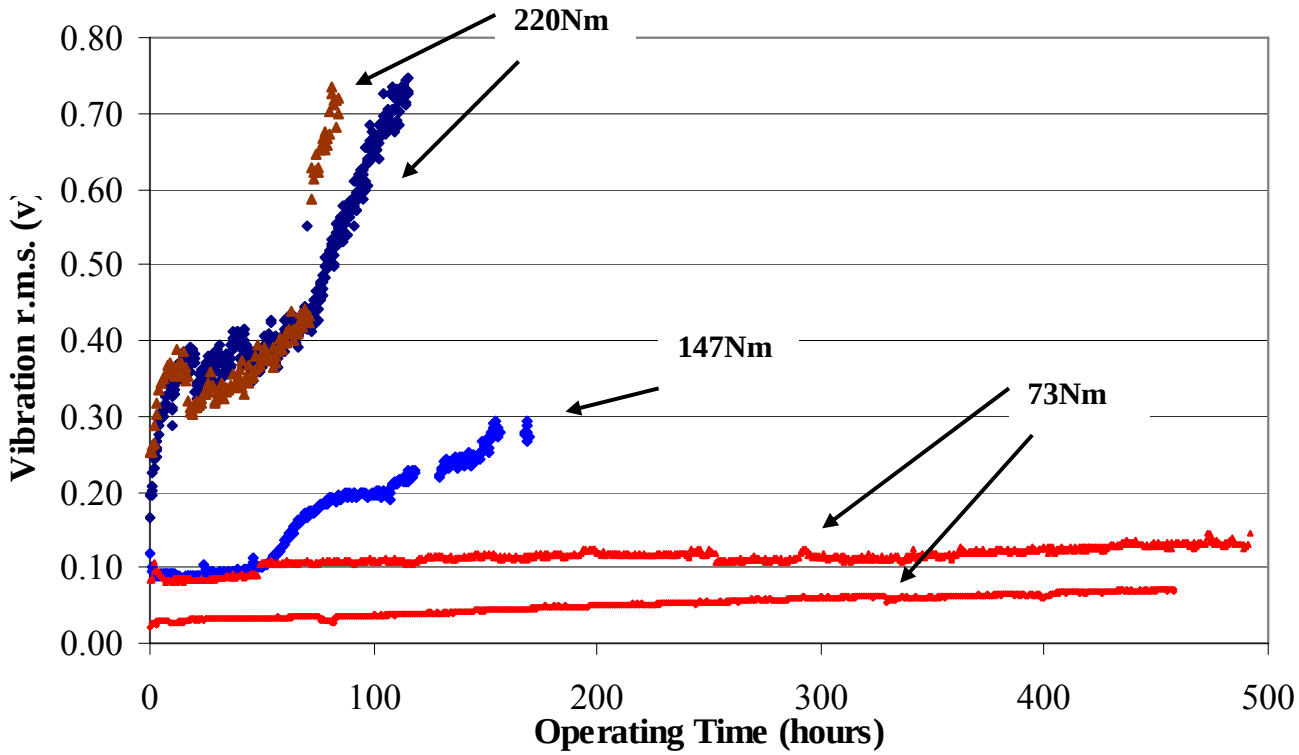

Figure 16 **Vibration r.m.s against gearbox operating time for various torque conditions at 745rpm**

From figure 16 it is clear that the highest applied torque resulted in the steepest rise in vibration r.m.s levels. This was expected as the higher applied torque produced higher pitting rates, which will modify the Hertzian contact zone at a faster rate. Furthermore, from figure 16 it was apparent that vibrations levels for 220Nm and 147Nm showed similar patterns of pitting progression, see figures 7 and 26 of Appendix B, i.e., a steep rise in vibration levels at the start of the tests; a relative period of constant levels followed by a steep rise before termination of the tests. This pattern was observed for one of the tests at 73Nm, see figure 27 [73 (1)], however, the pattern was not mirrored for the

second test at 73Nm. It is interesting to note that though the data for vibration at 220Nm and 147Nm showed a ‘plateau region’ (steady vibration level even though pitting steadily increased during this period) the value of percentage gear pitted area at which the r.m.s rose above the plateau region varied; 30% at 220Nm, 20% at 147Nm and 40% at 73Nm, see figure 8 and 28 and 29 of appendix B. The response of vibration to gear pitted area was considerably less sensitive than AE at all torque levels.

6.3.1.4 Fe Concentration

The Fe concentration plots with respect to gearbox operating time, see figure 17, showed that the higher the applied torque, the steeper the gradients. It is important to note that at the torque value of 73Nm a period existed where Fe concentration changed relatively slowly with respect to the running time.

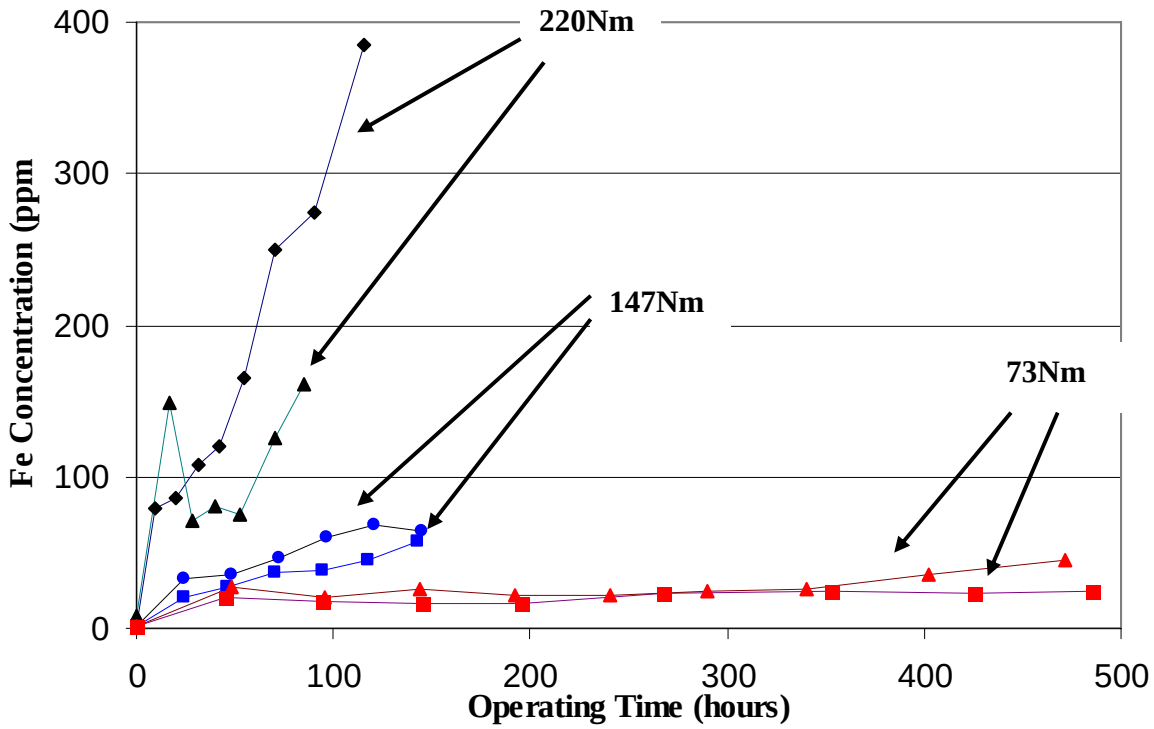

Figure 17 **Fe concentration against gearbox operating time for various torque conditions at 745 rpm**

6.3.2 What is the prognosis potential of these technique?

From the results presented it was clearly evident that the AE levels measured from the gear pinion could be linearly correlated to the gearbox pitting rates for all torque conditions, with detection of onset of pitting as early as 8% of the pitted area. This offered much earlier diagnosis than vibration analysis where only after between 20 to 40% of pitted area did this technique offer capability for defect identification. It was interesting to note that measurements of AE levels from the bearing casing suggested better sensitivity to pitting progression than vibration but only at the higher torque level

of 220Nm. This near linear relationship between AE (measured from the pinion) and pit progression offers great potential, and opportunities, for prognostics in rotating machinery. At high applied torque condition, the SOA technique performed better in pit growth monitoring in comparison to vibration technique. The disappointing performance of SOA and vibration at the lowest torque condition was not mirrored by the AE technique.

7 CONCLUSIONS

1. Fatigue gear testing was performed on spur gears to investigate the pitting detection capability of the AE, vibration and SOA techniques.
2. Higher applied torques resulted in greater pitting rate.
3. For all 3 indicators; Fe concentration, AE and vibration r.m.s, the rate of change of these parameters with respect to gearbox operating time increased with increasing applied torque.
4. AE r.m.s levels from the pinion were linearly correlated to pitting rates for all torque conditions.
5. AE levels from the bearing casing showed better sensitivity than vibration at only the higher toque level (220Nm). Vibration showed better sensitivity to pitting rates at the lower torque levels of 147 and 73Nm.
6. SOA technique has a better pit growth monitoring capability at the higher applied torques in comparison to vibration. However, both techniques showed less sensitivity at the lowest torque condition.

7. The linear relationship between AE, gearbox running time and pit progression implied that the AE technique offers good potential for prognostic capabilities for health monitoring of rotating machines. This will be the subject of future publication.

REFERENCES

1. Miller, R.K. and McIntire, P. Acoustic Emission Testing, Volume 5, 2nd ed., Non-destructive Testing Handbook. Ed., American Society for Non-destructive Testing, pp 275-310, 1987.
2. Toutountzakis, T. and Mba, D. Observation of Acoustic Emission Activity During Gear Defect Diagnosis. NDT and E International. **Vol. 36, No.7**, pp 471-477. 2003.
3. Mba, D. and Bannister, R.H. Condition monitoring of low-speed rotating machinery using stress waves: Part1 and Part 2. Proc Inst Mech Engrs. **Vol 213, Part E**, pp 153-185. 1999.
4. Holroyd, T. and Randall, N. The Use of Acoustic Emission for Machine Condition Monitoring. British Journal of Non-Destructive Testing. **Vol. 35(2)**, pp 75. 1992.
5. Mba D. The detection of shaft-seal rubbing in large-scale turbines using acoustic emission. 14th International Congress on Condition Monitoring and Diagnostic Engineering Management (COMADEM'2001). Manchester, UK, 4-6 September 2001. pp 21-28, ISBN 0080440363. 2001.

6. Mba, D. Applicability of acoustic emissions to monitoring the mechanical integrity of bolted structures in low speed rotating machinery: case study. NDT and E International. **Vol 35, No. 5**, pp. 293-300. 2002.
7. Mba, D., Cooke, A., Roby, D. and Hewitt, G. Opportunities offered by acoustic emission for shaft-seal rubbing in power generation turbines; a case study sponsored by the British Institute of NDT. International Conference on Condition Monitoring. Oxford, UK, 2-4 July 2003. pp 280-286, ISBN 1901892174. 2003.
8. Tandon, N. and Mata, S. Detection of Defects in Gears by Acoustic Emission Measurements, Journal of Acoustic Emission. **Vol. 17**, Issue 1-2, 23-27, 1999.
9. Singh, A., Houser, D. R., and Vijayakar, S. Early Detection of Gear Pitting, Power Transmission and Gearing Conference, ASME. **DE-Vol. 88**, 673-678, 1996.
10. Singh, A., Houser, D. R., and Vijayakar, S. Detecting Gear Tooth Breakage Using Acoustic Emission: A Feasibility and Sensor Placement Study, Journal of Mechanical Design. **Vol. 121**, 587-593, 1999.
11. Toutountzakis, T., Tan, C.K. and Mba, D. Application of acoustic emission to seeded gear fault detection. NDT and E International. **Vol. 38, No. 1**, pp 27-36. 2005.
12. Gadd, P. and Mitchell, P.J. Condition monitoring of helicopter gearboxes using automatic vibration analysis techniques. AGARD CP 369. Gears and power transmission system for helicopter turboprops. 29/1 – 29/10. 1984.
13. Leblanc, J.F.A., Dube, J.R.F. and Devereux, B. Helicopter gearbox vibration analysis in the Canadian Forces-applications and lessons. 1st International Conference, Gearbox noise and vibration. IMechE, Cambridge, UK. C404/023, pp 173 -177. 1990.

14. Cameron, B.G. and Stuckey, M.J. A review of transmission vibration monitoring at Westland Helicopter Ltd. 20Th European Rotorcraft Forum. Paper 116. pp 116/1 – 116/16. 1994.

15. Anderson, D.P., Lukas, M. and Yurko, R.J. Recent improvements in oil analysis spectrometers. International Conference on Condition Monitoring. Swansea, UK. 395-402. 1999.

16. Holroyd, T.J. (2000). Acoustic emission and ultrasounics. 1st ed. Coxmoor Publishing Company. Oxford, UK.

17. Tan, C.K. and Mba, D.U. Identification of the Acoustic Emission source during a comparative study on diagnosis of a spur gearbox. Tribology International. Volume 38, Issue 5, *Pages 469-480* , May 2005

18. Yesilyurt, I., Gu, F.S. and Ball, A.D. Gear tooth stiffness reduction measurement using modal analysis and its use in wear fault severity assessment of spur gears. NDT & E International. **Vol. 36, No. 5.** 357-372. 2003.

19. Choy, F.K., Polyschchuk, V., Zakrajsek, J.J., Handschuh, R.F. and Townsend, D.P. Analysis of the effects of surface pitting and wear omn the vibration of a gear transmission. Tribology International. **Vol. 29(1).** 77-83. 1996.

20. Drosjack, M.J. and Houser, D.R. An experimental and theoretical study of the effects of simulated pitch line pitting on the vibration of a geared system. ASME report 77-DET-123. 1977.

21. Fitch, J.C. Best Practices in maximising fault detection in rotating equipment using WDA. International Conference on Condition Monitoring. Swansea, UK. 65-75. 1999.

22. Davis A.M. Fundamental principles in setting alarms and limits in WDA. Practicing Oil Analysis. 2003.
23. Xiao, L., Rosen, B.G., Amini, N. And Nilsson, P.H. A study on the effect of surface topography on rough friction in roller contact. Wear. Vol 254(11), 1162-1169. 2003.
24. Diei, E.N. Investigation of the milling process using acoustic emission signal analysis, *PhD. Thesis*, Department of Mechanical engineering, University of California, Berkeley, CA. 1985.
25. Suh, N.P. Tribophysics. Prentice-Hall. Englewood Cliffs. NJ. 1986.
26. Dornfeld, D. and Handy, C. Slip detection using acoustic emission signal analysis. IEEE. 1868-1875. 1987.
27. MacBride, S.L., Bones, R.J., Sobczyk, M and Viner, M.R. Acoustics emission from lubricated and rubbing surfaces. Journal of Acoustic Emission. 8(1-2). 192-196. 1989.
28. Chee Keong Tan and David Mba, Limitation of Acoustic Emission for identifying seeded defects in gearboxes. Journal of **Non-Destructive Evaluation**, Vol. 24, No. 1, March 2005, p 11 - 28. ISSN: 0195-9298.
29. C K Tan and D Mba, Correlation between Acoustic Emission activity and asperity contact during meshing of spur gears under partial elastohydrodynamic lubrication., TRIBOLOGY LETTERS, 2005. ***In Press***

Appendix A

Pitting Progression for applied torque of 220 Nm

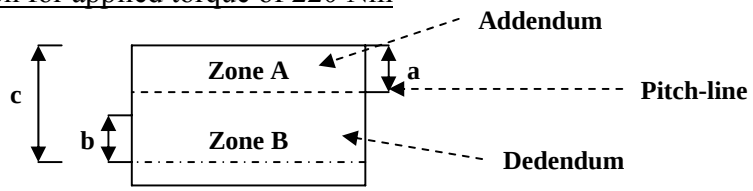

* All dimensions in mm.

Time Interval (hours)	220-Test 1		Time Interval (hours)	220-Test 2	
	Zone A	Zone B		Zone A	Zone B
9	Wear-in marks a = 3	Light pitting across face width b < 0.5 c = 5	0		
20	Scoring marks a = 2	Pitting moving towards pitch-line. Similar no. of pits but deeper in depth 0.5 < b < 1 8.3% pitting area c = 5	17	Scoring marks a = 2.5	Light pitting across face width b = 0.5 8.3% pitting area c = 5
31	Scoring marks a = 2.5	Pitting moving towards pitch-line. Pits are deeper and bigger b = 1 (cover about ¾ of this range) 12.5% pitting area c = 5	28	Scoring marks a = 2.5	Pitting moving towards pitch-line. Pits are deeper and bigger b = 1 (cover about ¾ of this range) 12.5% pitting area c = 5
41	Scoring marks a = 2.5	Pitting moving towards pitch-line. Pits are bigger and deeper b = 1.5 (cover about ¾ of this range) 18.8% pitting area c = 5	40	Scoring marks a = 2.5	Pitting moving towards pitch-line. Pits are bigger and deeper b = 1.5 (cover about 2/3 of this range) 16.7% pitting area c = 5
54	Scoring marks a = 2.5	More pitting and pits touched the pitch-line b = 2 (cover about 2/3 of this range) 22.2% pitting area c = 5	52	Scoring marks a = 2.5	More pitting and pits touch the pitch-line b = 2 (cover about 3/4 of this range) 25.0% pitting area c = 5
70	Scoring marks a = 2.5	Pitting moving downward to the dedendum. More pits b = 2 33.3% pitting area c = 6	70	Scoring marks a = 2.5	Pitting moving downward to the dedendum. More pits b = 2.5 (cover about 5/6 of this range) 34.7% pitting area c = 5.5
91	Scoring marks a = 3	Pits touched the pitch-line and spread across the face width b = 2.5 (cover about 7/8 of this range) 36.5% pitting area c = 6	86	Scoring marks a = 2.5	Pits reached the pitch-line and spread across the face width b = 3 (cover about 9/10 of this range) 45.0% pitting area c = 5.5
116	Scoring marks a = 3	Almost every tooth has large pits across face width and reached the pitch-line b = 3, 50.0% pitting area c = 6			

Pitting Progression for applied torque of 147 Nm

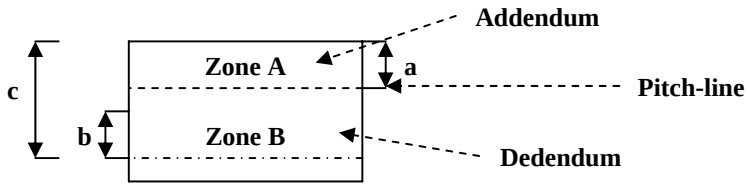

* All dimensions in mm.

Time Interval (hours)	147-Test 1		Time Interval (hours)	147-Test 2	
	Zone A	Zone B		Zone A	Zone B
24	Wear-in marks a = 3	Light pitting across half the face width b < 0.5 4.2% pitting area c = 4.5	24	Wear-in marks a = 3.5	Light pitting across one quarter the face width b = 1 (cover about 1/4 of this range) 4.2% pitting area c = 5
46	Wear-in marks a = 3	Pitting moving towards pitch-line. Some teeth have pitting at addendum b= 1 16.7% pitting area c = 5	48	Wear-in marks a = 3..5	Pitting moving towards pitch-line. Very deep pits along the bottom. b = 1.5 (cover about 7/12 of this range) 14.6% pitting area c = 5.5
70	Wear-in marks a = 3	Pitting moving towards pitch-line. b = 1.5 25.0% pitting area c = 5	72	Wear-in marks a = 3.5	Pitting moving across face width, deeper pits at lower regions. b = 1.5 25.0% pitting area c = 5.5
94	Wear-in marks a = 3	Pitting moving towards pitch-line. b = 2 33.3% pitting area c = 5	96	Wear-in marks a = 3.5	Pitting moving towards pitch-line. More teeth with increased no. and deeper pits at the addendum. b = 2 33.3% pitting area c = 5.5
118	Wear-in marks a = 3	Pitting moving towards pitch-line. b = 2.5 41.7% pitting area c = 5	121	Wear-in marks a = 2.5	Pitting moving towards pitch-line. More teeth with deeper pits at the addendum. b = 2.5 41.7% pitting area c = 5.5
143	Wear-in marks a = 2.5	Pitting reached pitch-line b = 3 50.0% pitting area c = 5.5	145	Scoring marks a = 2.5	Pitting moving reached pitch-line. Some teeth with very deep pitting at the addendum. b = 3 50.0% pitting area c = 5.5

Pitting Progression for applied torque of 73 Nm

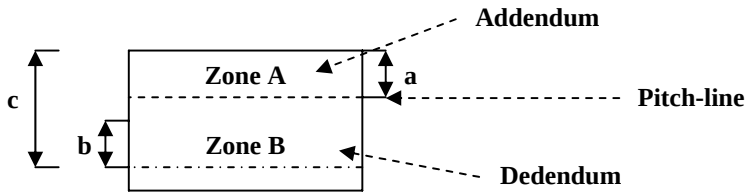

* All dimensions in mm.

Time Interval (hours)	73-Test 1		Time Interval (hours)	73-Test 2	
	Zone A	Zone B		Zone A	Zone B
45	Wear-in marks a = 3	Light pitting across half the face width b < 0.5 c = 5	49	Wear-in marks a = 2.5	Light pitting across one quarter of the face width. Some teeth have pitting at addendum. b= 1.5 (cover about 1/4of this range) 6.3% pitting area c = 5
95	Wear-in marks a = 3	Pitting moving towards pitch-line and occupied half of the face width. b= 1 (cover about ½ of this range) 8.3% pitting area c = 5	96	Wear-in marks a = 2.5	Pitting moving across pitch-line and occupied half of the face width. b= 1.5 (cover about ½ of this range) 12.5% pitting area c = 5.5
145	Wear-in marks a = 3	Pitting moving towards pitch-line and concentrated pitted on the right 1/3 of face width. b = 2 (cover about 1/3 of this range) 11.1% pitting area c = 5	144	Wear-in marks a = 2.5	Pitting moving across pitch-line and occupied 2/3 of the face width. Pits got deeper. b= 1.5 (cover about 2/3 of this range) 16.7% pitting area c = 5.5
196	Wear-in marks a = 3	Pitting moving towards pitch-line and concentrated pitted on the right 1/3 of face width. b = 2.5 (cover about 1/3 of this range) 13.9% pitting area c = 5.5	193	Wear-in marks a = 2.5	Pitting moving across pitch-line and occupied the whole of face width. b = 1.5 (cover about 1/3 of this range) 25.0% pitting area c = 5.5
268	Wear-in marks a = 3	Pitting moving towards pitch-line. b = 1.5 full face width & b = 1 (cover about 1/3 of this range) 30.6% pitting area c = 5.5	241	Wear-in marks a = 2.5	Pitting moving towards pitch-line. Almost all teeth has 25% pitting area, the rest has 27.8%. Some pitting over pitch-line b = 2.5 (cover about 2/3 of this range) 27.8% pitting area c = 5.5
353	Wear-in marks a = 3	Pitting moving towards pitch-line. Only 3 to 4 teeth have this pitting area. b = 1.5 half face	290	Wear-in marks a =2.5	Pitting moving towards pitch-line. Pitch-line covered with pits b = 2.5 (cover about 6/7 of this range)

		width & b = 2.5 half face width 33.3% pitting area c = 5.5			35.7% pitting area c = 5.5
425	Wear-in marks a = 3	Pitting moving towards pitch-line. 6 to 8 teeth have this pitting area. b = 1.5 half face width & b = 2.5 half face width 33.3% pitting area c = 5.5	341	Wear-in marks a = 2.5	Pitting reached pitch-line. Almost all teeth have 33.3% pitting area, only a few teeth have 41.7%. b = 2.5 41.7% pitting area c = 5.5
485	Wear-in marks a = 3	Pitting moving towards pitch-line. 11 to 15 teeth have this pitting area. b = 1.5 half face width & b = 2.5 half face width 33.3% pitting area c = 5.5	403	Wear-in marks a = 2.5	The no. of teeth with 41.7% pitted area has increased from a few to 50% of the total no. of gear teeth. b = 2.5 41.7% pitting area c = 5.5
			472	Wear-in marks a = 2.5	Most teeth have 41.7% of gear pitted area, others reached 50%. b = 3 50.0% pitting area c = 5.5

* The test was terminated since the pitting area did not increase, but this percentage of pitted area was spreading across all the rest of gear teeth. This implied localised pitting has been developed into distributed pitting.

Appendix B

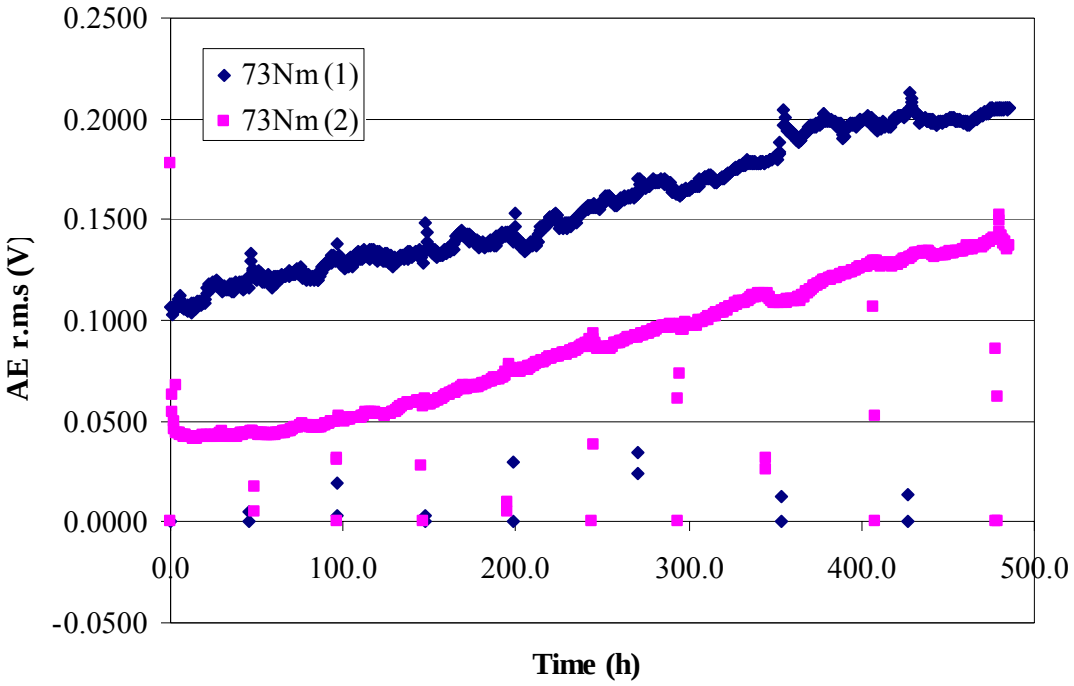

Figure 18 AE r.m.s. against operating time at 73 Nm; 745 rpm

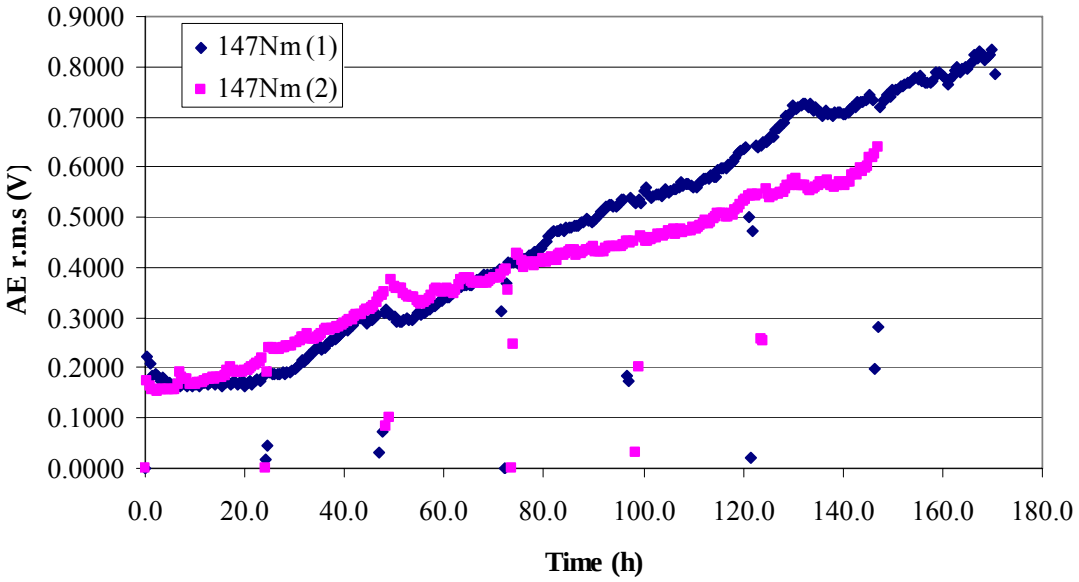

Figure 19 AE r.m.s against operating time at 147 Nm; 745 rpm

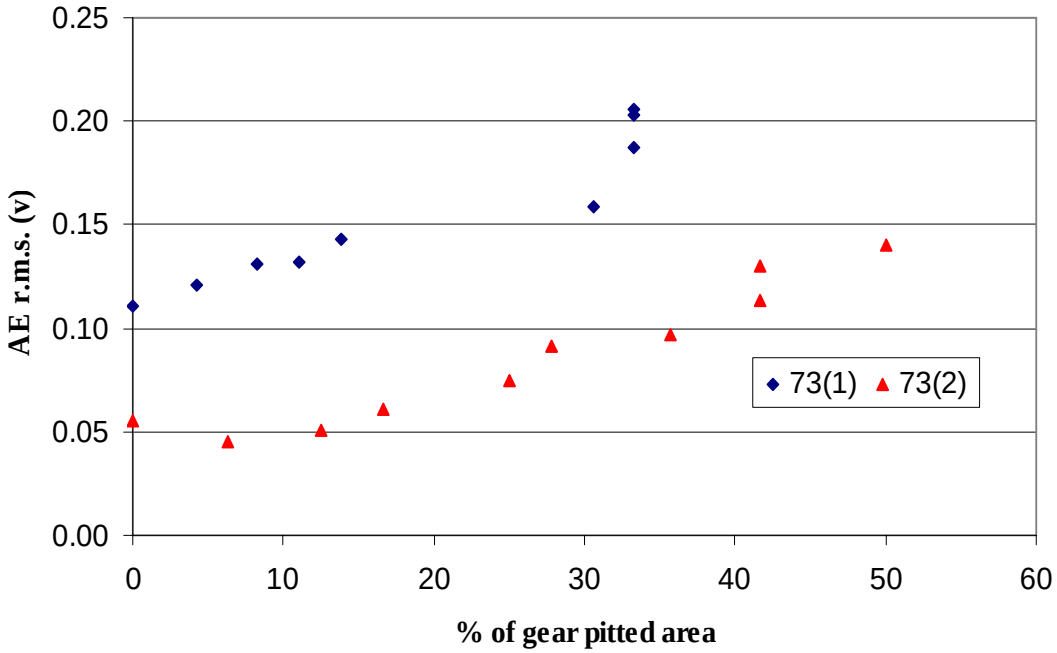

Figure 20 **AE r.m.s against % pitted area; 73 Nm, 745 rpm**

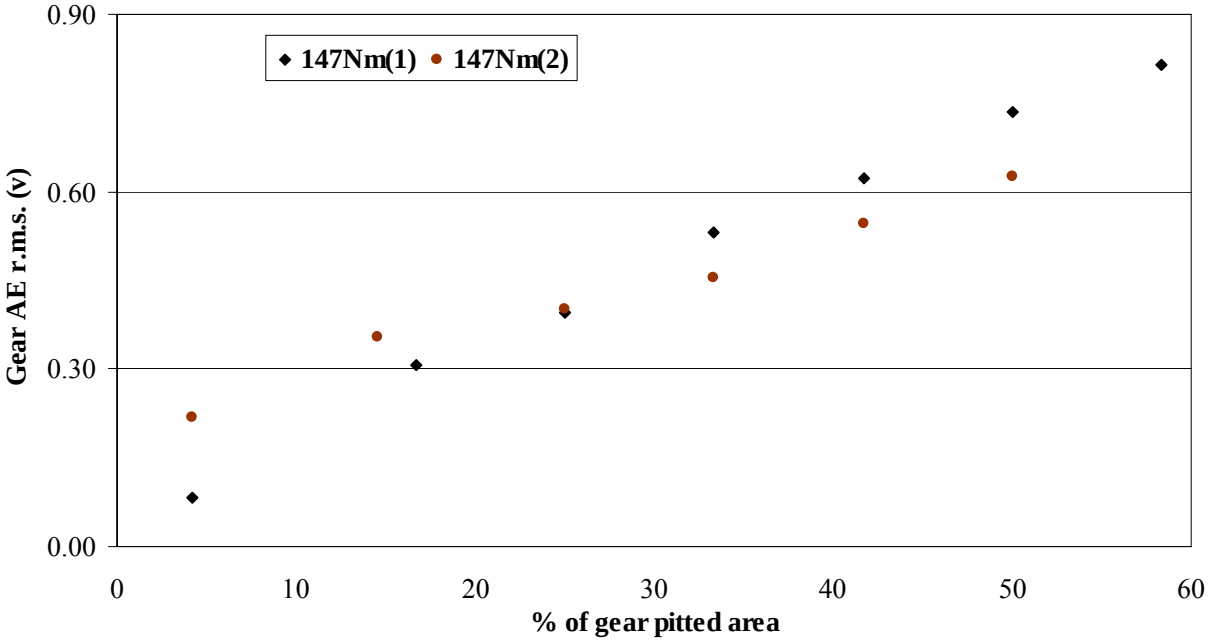

Figure 21 **AE r.m.s against % pitted area; 147 Nm, 745 rpm**

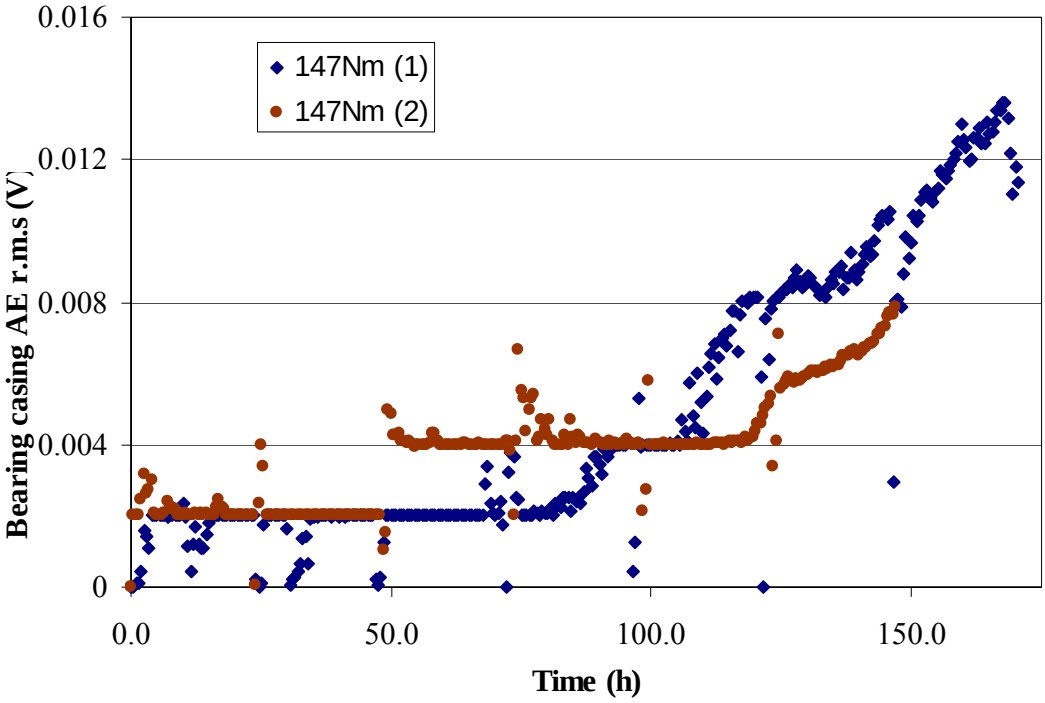

Figure 22 Bearing casing AE r.m.s against operating time at 147 Nm; 745 rpm

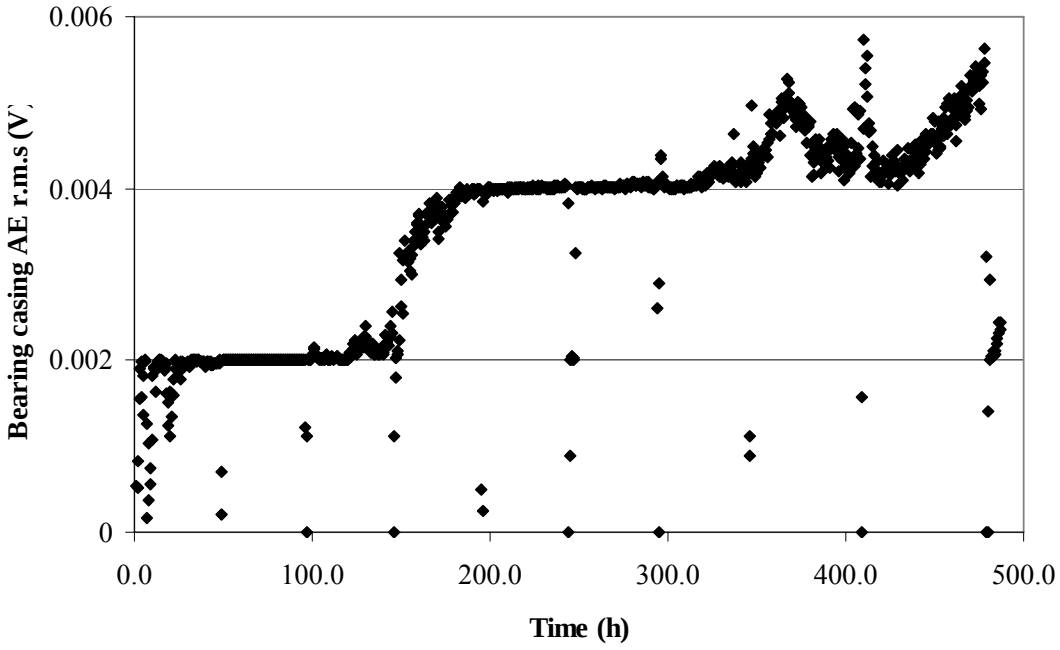

Figure 23 Bearing casing AE r.m.s against operating time at 73 Nm; 745 rpm

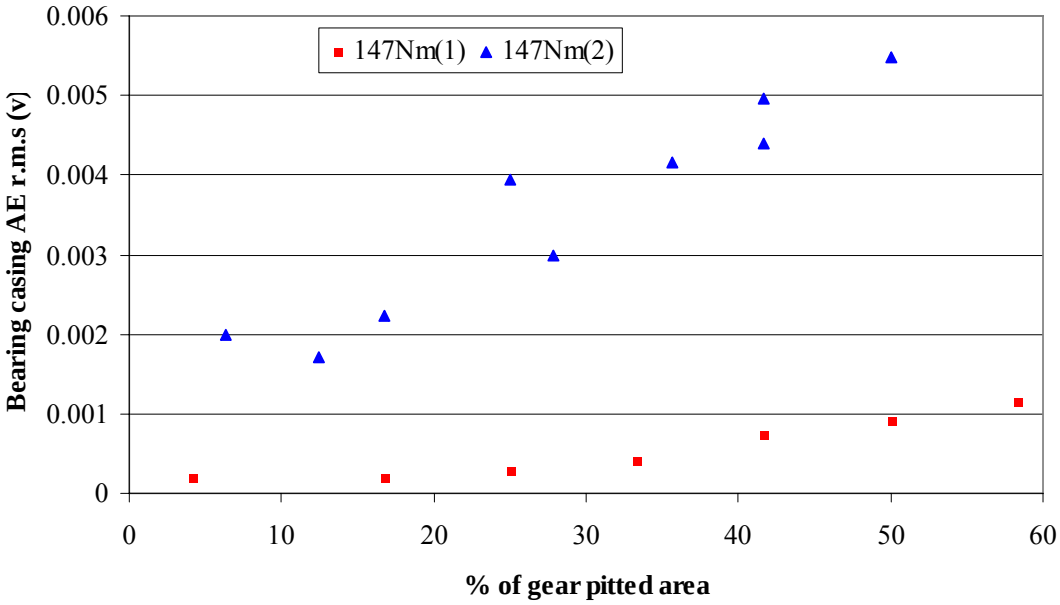

Figure 24 Bearing casing AE r.m.s against % pitted area; 147 Nm, 745 rpm

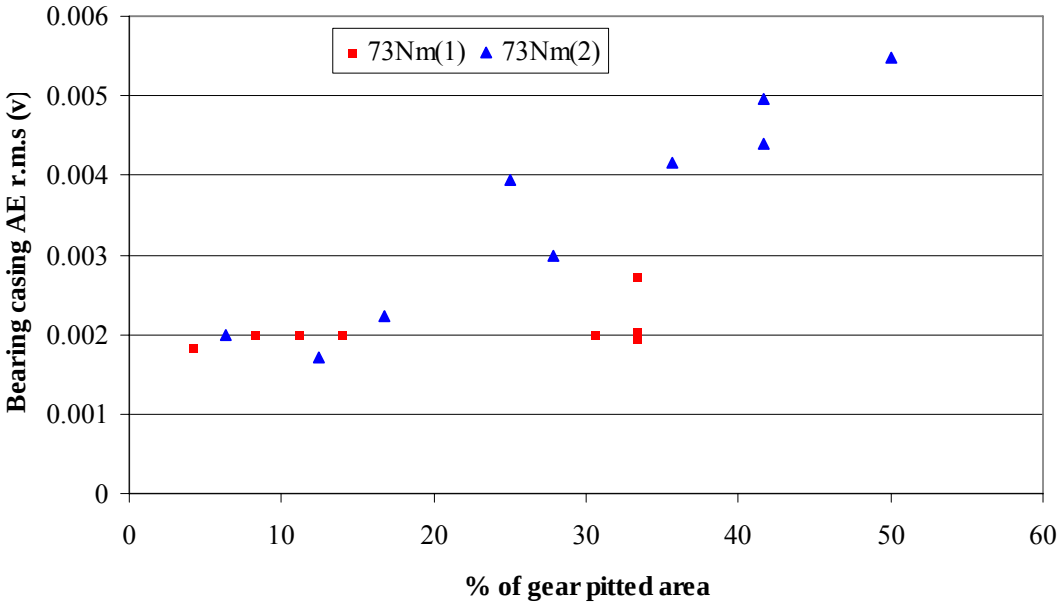

Figure 25 Bearing casing AE r.m.s against % pitted area; 73 Nm, 745 rpm

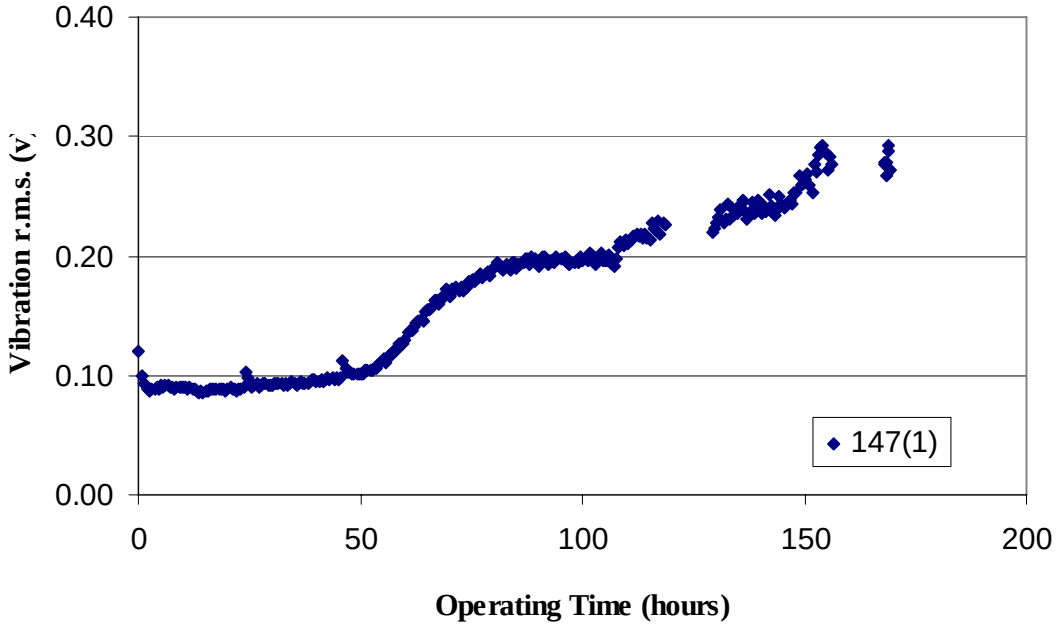

Figure 26 **Vibration r.m.s against operating time at 147 Nm; 745 rpm**

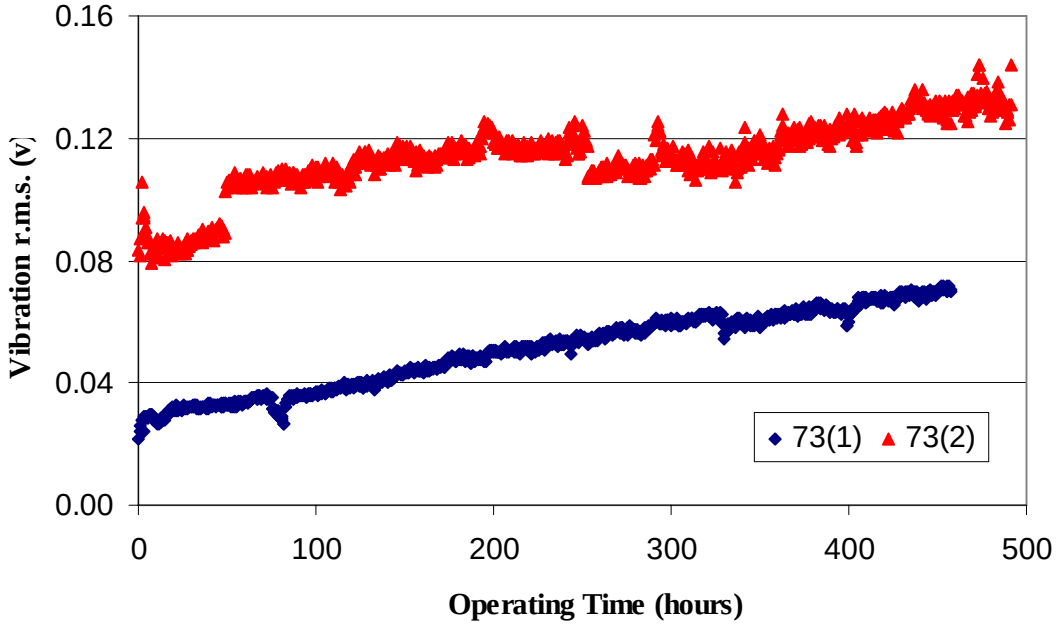

Figure 27 **Vibration r.m.s. against operating time at 73 Nm; 745 rpm**

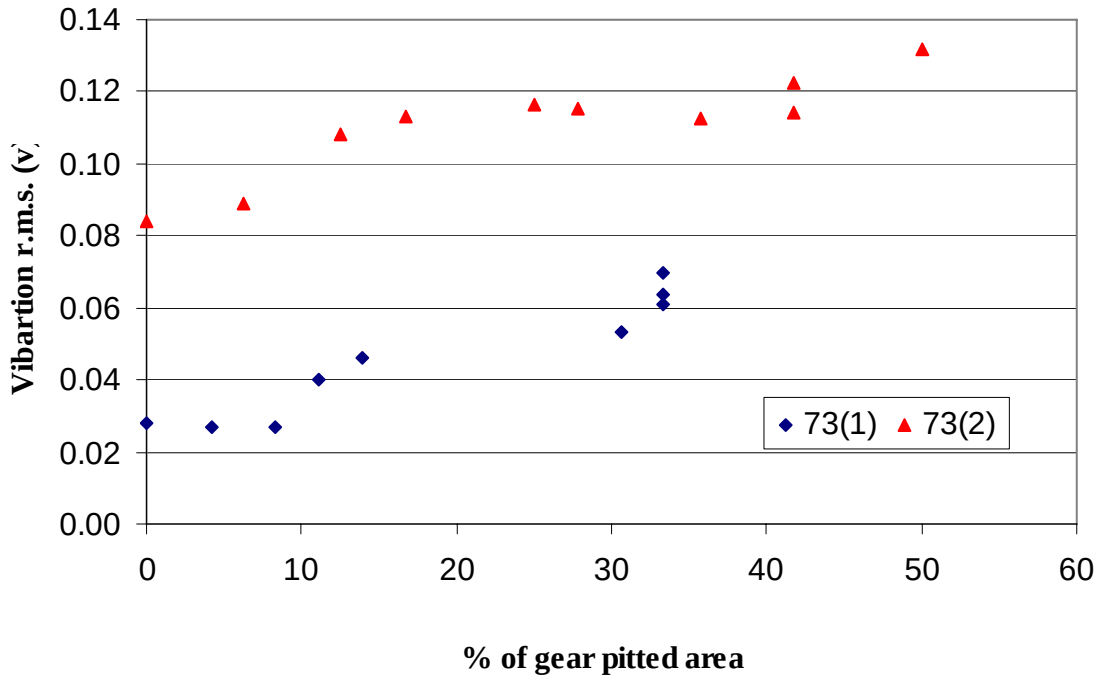

Figure 28 **Vibration r.m.s against % pitted area; 73 Nm, 745 rpm**

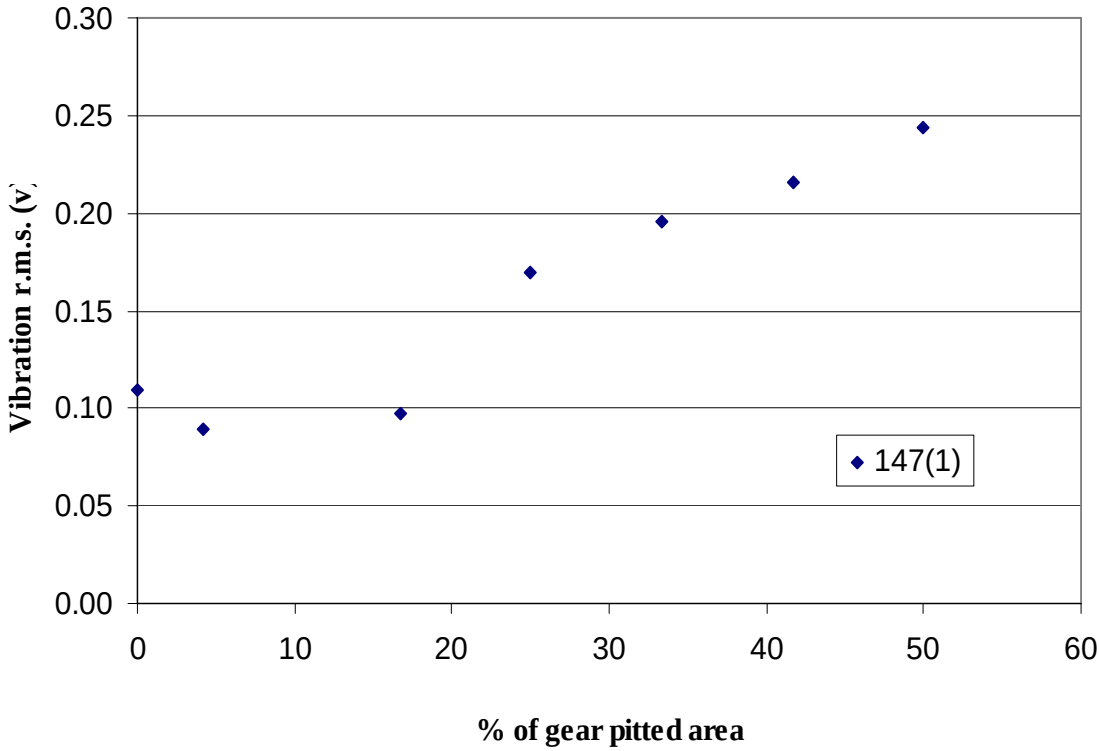

Figure 29 **Vibration r.m.s against % pitted area; 147 Nm, 745 rpm**

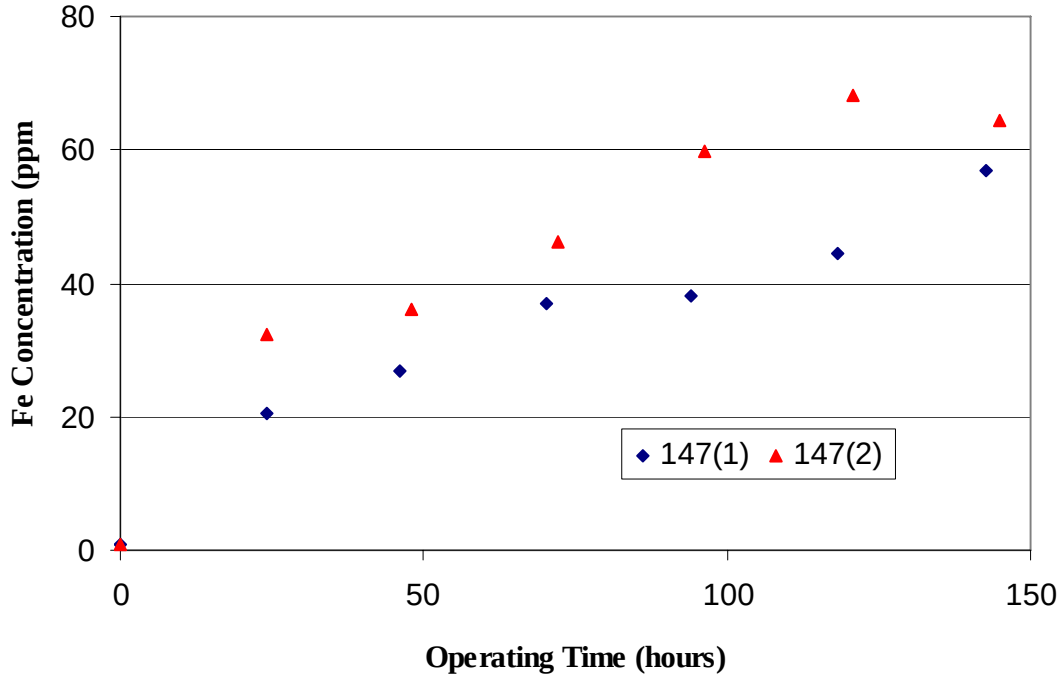

Figure 30 **Fe concentration with correction against operating time at 147 Nm; 745 rpm**

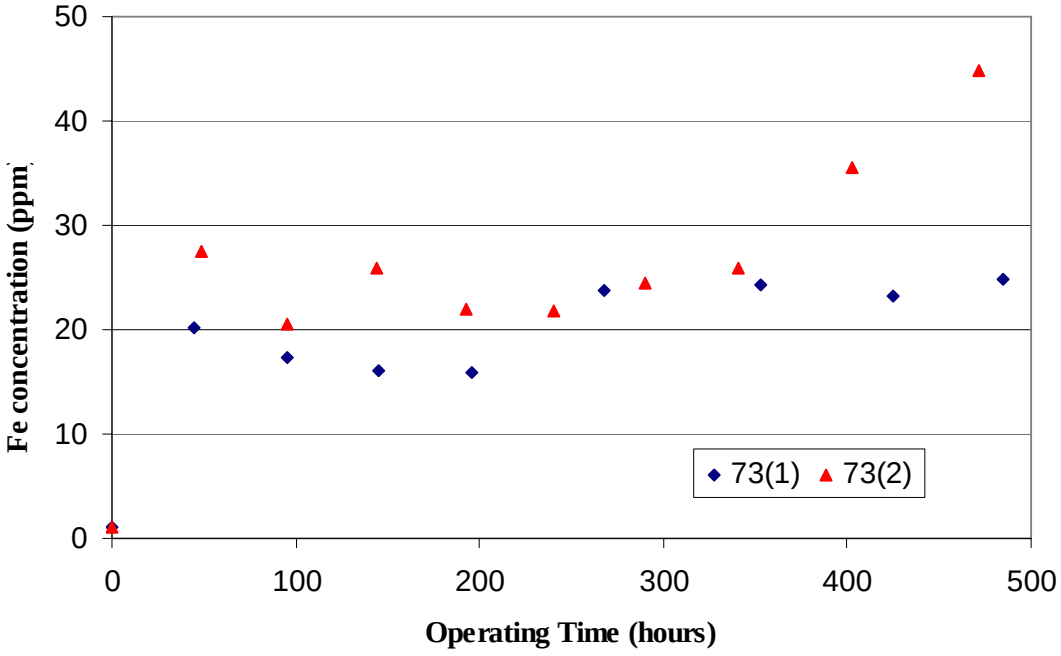

Figure 31 **Fe concentration with correction against operating time at 73 Nm; 745 rpm**

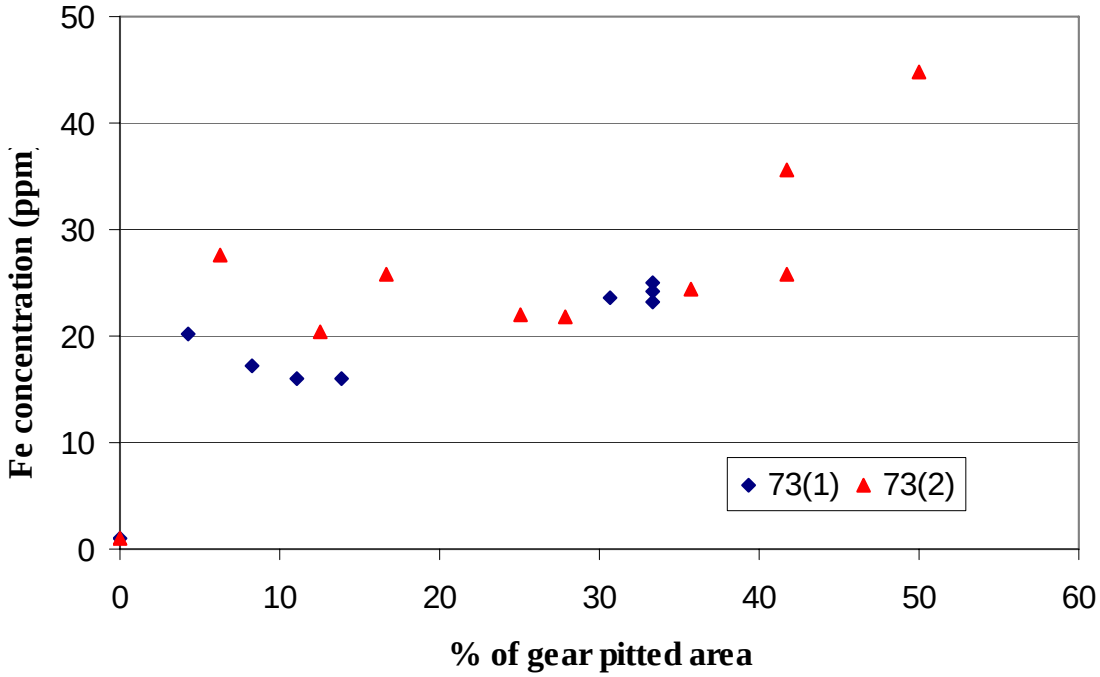

Figure 32 **Fe concentration with correction against % pitted area; 73 Nm, 745 rpm**

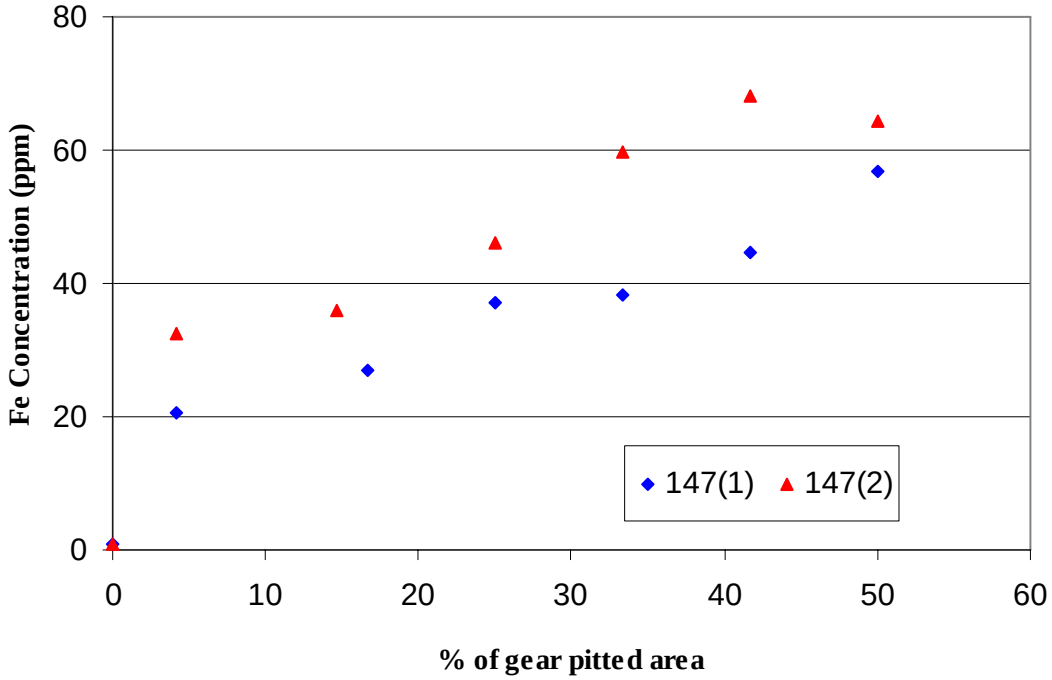

Figure 33 **Fe concentration with correction against % pitted area; 147 Nm, 745 rpm**